P-04-107

Forsmark site investigation

Interpretation of petrophysical data from the cored boreholes KFM01A, KFM02A, KFM03A and KFM03B

Håkan Mattsson, Hans Thunehed, Hans Isaksson
GeoVista AB

Lutz Kübler, Sveriges Geologiska Undersökning

November 2004

Svensk Kärnbränslehantering AB
Swedish Nuclear Fuel
and Waste Management Co
Box 5864
SE-102 40 Stockholm Sweden
Tel 08-459 84 00
+46 8 459 84 00
Fax 08-661 57 19
+46 8 661 57 19

ISSN 1651-4416
SKB P-04-107

Forsmark site investigation

Interpretation of petrophysical data from the cored boreholes KFM01A, KFM02A, KFM03A and KFM03B

Håkan Mattsson, Hans Thunehed, Hans Isaksson
GeoVista AB

Lutz Kübler, Sveriges Geologiska Undersökning

November 2004

Keywords: Petrophysics, Anisotropy, Magnetic susceptibility, AMS, Density, Porosity, Resistivity, Induced polarisation, Gamma-ray spectrometry, AP PF-400-03-48, AP PF-400-03-91, Field note no Forsmark 336.

Abstract

This document reports the interpretation of petrophysical data from the cored boreholes KFM01A, KFM02A, KFM03A and KFM03B in the Forsmark site investigation area.

The petrophysical determinations include magnetic susceptibility, remanent magnetization, anisotropy of magnetic susceptibility (AMS), density, porosity, electric resistivity, induced polarization and gamma-ray spectrometry.

Some deviating results from what is normal in the rock types are listed below:

- Vuggy granite/episyenite samples have high porosity, low density, low magnetic susceptibility and low resistivity. They show a relation between resistivity and porosity that indicates the presence of vugs, constrictions, dead-end pores and/or crocked path-ways.
- The median porosity is highest in KFM03A and lowest in KFM01A.
- Resistivity of samples in fresh water is strongly dependent upon surface conductivity. Samples with fine-grained phyllosilicates seem to have the lowest resistivities, vuggy granite/episyenite samples excluded.
- One metagranite sample of KFM01A (depth c 476 m) has a significantly lower magnetic susceptibility but a slightly higher density than the other metagranite samples in this borehole.
- The magnetic fabric orientation of KFM03 clearly deviates from the fabric orientations of KFM01 and KFM02, with shallow to moderate dips of the foliation in KFM03 compared to moderate to steep dips in KFM01 and KFM02.
- In general, the metagranite-granodiorite displays normal values for granite that is; in average 2.9% potassium, 5 ppm uranium and 17 ppm thorium. For other rock types, the samples are too few to draw statistical conclusions.
- The episyenite samples and a metagranite-granodiorite sample close to the episyenite, in the upper part of KFM02A, show a relative enrichment in potassium and thorium, 4.2–4.6% K and 19–23 ppm Th, respectively.
- Some metagranite samples show high thorium levels, 29 and 42 ppm.
- A leucogranite and a pegmatite granite sample in KFM03 show typically high content of potassium, uranium and thorium.

Sammanfattning

Denna rapport beskriver tolkningen av petrofysiska data från kärnborrhålen KFM01A, KFM02A, KFM03A och KFM03B i Forsmarksområdet.

Den petrofysiska informationen omfattar magnetisk susceptibilitet, remanent magnetisering, den magnetiska susceptibilitetens anisotropi (AMS), densitet, porositet, elektrisk resistivitet, inducerad polarisation och gammaspektrometri.

Några resultat som avviker mot vad som är normalt för bergarterna är som följer:

- Prov av porös granit/episyenit uppvisar hög porositet, låg densitet, låg magnetisk susceptibilitet och låg resistivitet. Proven uppvisar därutöver en relation mellan resistivitet och porositet som indikerar förekomst av hålrum, avsnörda porer, slutna porer och/eller vindlande porvolymer.
- Medelporositeten är högst i KFM03A och lägst i KFM01A.
- Resistiviteten av prov i färskvatten är starkt beroende av ytledningsförmågan. Prov som innehåller finkorniga fyllosilikater har synbarligen lägst resistivitet, den porösa graniten/episyeniten undantagen.
- Ett prov av metagranit-granodiorit från KFM01A (ca 476 m djup) uppvisar signifikant lägre magnetisk susceptibilitet och en något högre densitet än övriga prov av metagranit i detta borrhål.
- Orienteringen av de magnetiska mineralen, deras struktur och textur, i KFM03A avviker tydligt från orienteringen i KFM01 och KFM02. I KFM01 och KFM02 stupar foliationsplanen mestadels brant, medan de i KFM03 huvudsakligen har en flack stupning.
- Metagranit-granodiorit visar i allmänhet normala värden för granit; i detta fall i medeltal 2.9 % kalium, 5 ppm uran and 17 ppm torium. För övriga bergarter är underlaget för litet för att dra statistiska slutsatser.
- Prov av episyenit och näraliggande prov av metagranit-granodiorit i övre delen av KFM02A uppvisar en relativ anrikning av kalium och torium, 4.2–4.6 % K respektive 19–23 ppm Th.
- Vissa metagranitprov uppvisar förhöjda toriumvärden, 29 och 42 ppm.
- Ett prov av leucogranit och ett av pegmatitgranit från KFM03 uppvisar hög halt av kalium, uran och torium.

Contents

1 Introduction

This document reports the interpretation of petrophysical data from the cored boreholes KFM01A, KFM02A, KFM03A and KFM03B (Figure 1-1), which is one of the activities performed within the site investigation at Forsmark.

The petrophysical determinations include magnetic susceptibility, remanent magnetization, anisotropy of magnetic susceptibility (AMS), density, porosity, electric resistivity, induced polarization and gamma-ray spectrometry. The gamma-ray spectrometry measurements were performed by the Geological Survey of Sweden, whereas the other parameters were measured at the Petrophysical Laboratory of the Division of Applied Geophysics, Luleå University of Technology.

The interpretations presented in this report were conducted according to the activity plans AP PF-400-03-48 and AP PF-400-03-91 (SKB internal controlling documents), by Håkan Mattsson, Hans Thunehed and Hans Isaksson at GeoVista AB. Mikael Keisu at GeoVista AB was responsible for the data delivery. Lutz Kübler at the Geological Survey of Sweden was responsible for the gamma-ray spectrometry measurements.

Information on petrophysical properties on different rock types and their surface distribution in the Forsmark area have previously been reported in /1/ and /7/.

No field work has been performed.

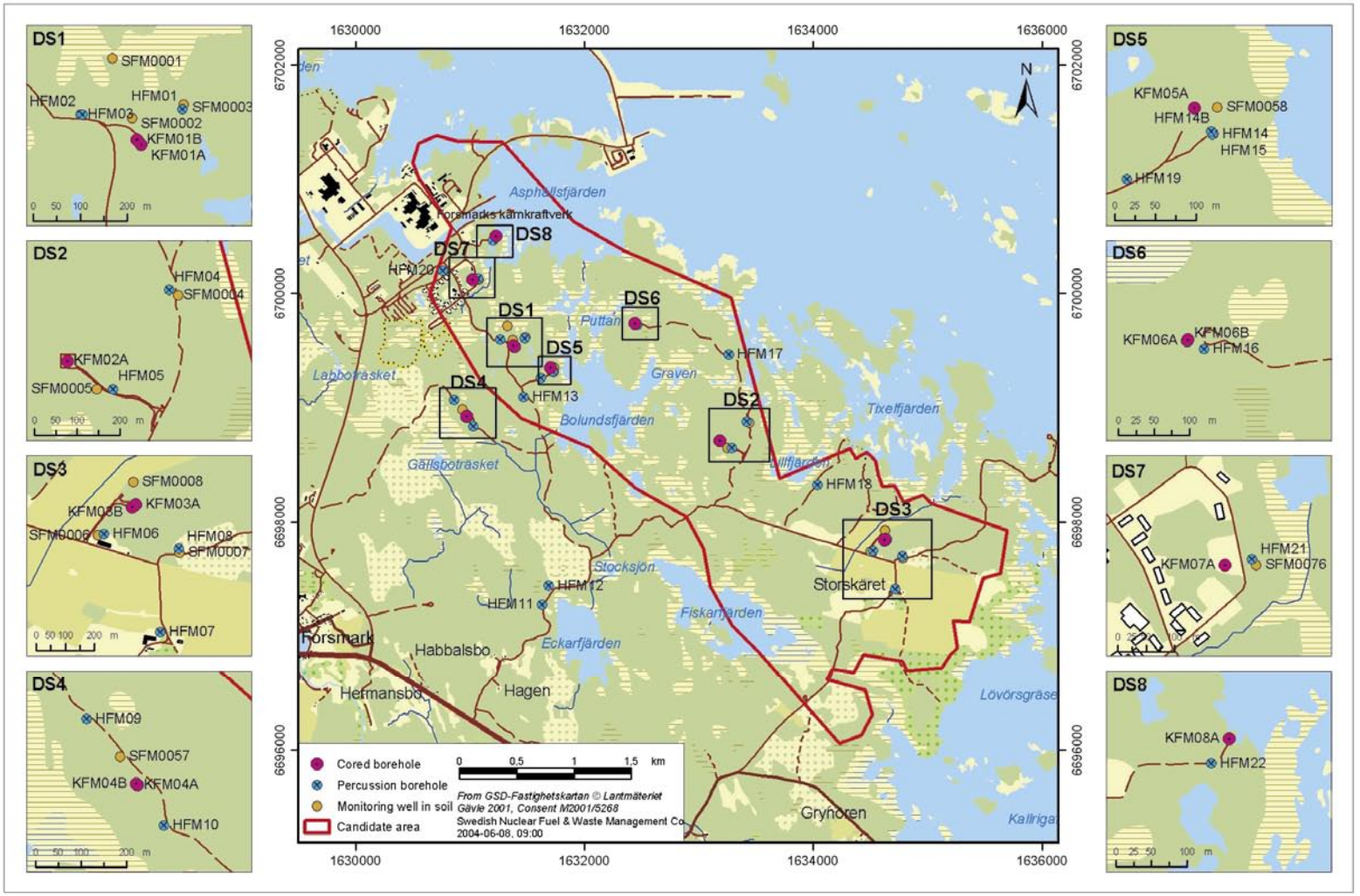

Figure 1-1. *Drill sites (DS) at Forsmark. KFM01A is situated at DS1, KFM02A at DS2 and KFM03A and KFM03B at DS3.*

2 Objective and scope

The purpose of petrophysical measurements is to gain knowledge of the physical properties of different rock types. This information is used to increase the understanding of geophysical logging measurements, to perform quality controls of the logging data and to support the geological core mapping. Rock fabric information and parameters related to grain size are also achieved from the petrophysical measurements.

The work comprises statistical processing and evaluation of results from measurements on core samples. Analyses were made regarding rock type characteristics and the distribution of the measured properties with respect to depth.

3 Sample handling and geological coding

In the following section, Section 3.1, the handling and geological coding of the samples taken for measurements of petrophysical parameters is described. The sampling for gamma-ray spectrometry was performed in a different manner, which is described in Section 3.2.

3.1 Petrophysical samples

Each petrophysical sample is a c 200 mm long split core with a diameter of c 50 mm. The samples were assigned an identity code comprising "borehole identity", "section up" and "section low". The samples were cut in two halves and electric measurements were performed on these. Four 22 mm long specimens were then drilled from each of the original core samples, perpendicular to the core axis. Each specimen was given a specimen number, to separate them from each other. The magnetic measurements were performed on single specimens. All specimens plus, if possible, the remains of the core sample were then assembled and the density (wet and dry) and porosity measurements were performed. A scheme showing the number and type of determinations per sample, for each borehole respectively is presented in Table 3-1. Measurement techniques and sample handling are described in more detail in /1/.

Table 3-1. Number and type of petrophysical determinations on each core sample from KFM01A, KFM02A, KFM03A and KFM03B.

Borehole	Number of samples	Density/ Porosity	AMS	Remanence	Resistivity/IP
KFM01A	10	1	4	4	2
KFM02A	13	1	4	4	2
KFM03A	9	2	4	1	2
KFM03B	1	2	4	1	2

The samples are not oriented with reference to any co-ordinate system, there is only a mark indicating section up and section low. The orientation of the remanence vectors and the principal anisotropy axes are therefore only made with reference to the core axis. Declination data of these parameters are consequently meaningless but inclination variations may be possible to interpret if the borehole is sub-vertical. The dip of KFM01A is c 74–85°, KFM02A is c 80–87°, KFM03A is c 82–87° and the dip of KFM03B is c 84–85°. The borehole dips are steep enough to allow a meaningful interpretation of inclination variations of the remanence vector and the principal anisotropy directions, with an accuracy of c ± 10–15°.

The selection of sampling (measurement) locations was performed in co-operation with the responsible geologist. Each sample was collected in the direct vicinity of geological samples taken for thin section analyses and geochemical analyses. This allows reliable comparisons between petrophysical and geological data. A geological coding system was established containing four major rock groups (A, B, C and D) and sub-groups of rock types for each rock group respectively. Each rock sample was classified according to this system, which is presented below.

Group A. Supracrustal rocks

A1. Felsic to intermediate metavolcanic and metavolcanoclastic rocks.

A2. Fe-rich mineralization.

A3. Veined gneiss (paragneiss?).

Group B. Ultramafic, mafic, intermediate and quartz-rich felsic (granitoid) meta-intrusive rocks

B1. Meta- ultramafic rock.

B2. Metagabbro.

B3. Metadiorite, quartz-bearing metadiorite, metadioritoid.

B4. Amphibolite.

B5. Metatonalite.

B6. Metatonalite to metagranodiorite.

B7. Metagranodiorite.

B8. Metagranodiorite to metagranite.

B9. Metagranite

B10. Metagranite, aplitic.

Group C. Quartz-rich felsic (granitoid) meta-intrusive rock, fine- to medium-grained. Occurs as dykes and lenses within rocks belonging to Groups A and B

(No subgroups).

Group D. Granite, pegmatitic granite, pegmatite. Occurs as dykes and minor intrusive bodies within rocks belonging to Groups A and B. Pegmatites display variable time relationships to Group C

D1. Granite.

D2. Pegmatitic granite.

D3. Pegmatite.

The core samples collected for analyses of density, porosity, magnetic, electric and electromagnetic properties include:

KFM01A

5 metagranite to granodiorite samples (B8; depths c 110 m, 317 m, 476 m, 706 m and 947 m), 2 amphibolite samples (B4; depths c 355 m and 474 m) and 3 group C samples. The group C samples include one metagranite (depth c 970 m), one metagranodiorite (depth c 242 m) and one metagranodiorite to tonalite (depth c 521 m).

KFM02A

8 metagranite to granodiorite or metagranite samples (B8 and B9; depths c 316 m, 317 m, 351 m, 712 m, 949 m, 953 m, 244 m and 350 m), 2 samples of very porous episyenite (depths c 263 m and 295 m), one sample of very porous metagranitoid (depth c 278 m) and 2 group C samples. The group C samples include one metagranite (depth c 552 m) and one metatonalite (depth c 916 m).

KFM03A and KFM03B

6 metagranite to granodiorite samples (B8; depths c 165 m, 432 m, 504 m, 619 m, 856 m and 957 m), one metatonalite (B5; depth c 239 m), one metatonalite (C; depth c 310 m) and one metagranite (D?; depth c 157 m). All samples above were collected in KFM03A. One sample of pegmatitic granite (D2; depth c 60 m) was collected in KFM03B.

3.2 Samples for gamma-ray spectrometry

Gamma-ray spectrometry was carried out on samples taken for geochemical analyses. The handling of these samples is described in /2/ and includes grinding. The spectrometry measurements were carried out on this grinded material.

From each sample, two 60 g fractions (sub-samples) were extracted and put into plastic pots, which were hermetically sealed and stored for three weeks awaiting isotope equilibrium.

The samples were given ID:s according to SKB standards (borehole ID, secup, seclow), the same ID:s as the corresponding geochemical samples. In addition, the samples were assigned a unique SGU-ID in order to separate the sub-samples. Geological coding of the samples was made as part of the work presented in /2/.

Measurements were made of each sub-sample according to the routines developed at the petrophysical laboratory of SGU. The measuring time was one hour and several samples were measured two, and in some cases three times for the purpose of reproducibility control. Background radiation was checked daily and after the measuring of every 10–15 samples, K, U and Th standards were measured.

3.3 Compilation of the sampling

The Tables 3-2 to 3-4 show the location of the samples for petrophysical measurements and gamma-ray spectrometry for each of the three boreholes, respectively.

Table 3-2. Petrophysical samples and samples for gamma-ray spectrometry from drillhole KFM01A.

Drillhole ID	Sec up (m)	Sec low (m)	Petro-physical sample	Gamma-ray spectrometry sample	Rock type
KFM01A	109.60	110.06		X	metagranite-granodiorite
KFM01A	110.06	110.26	X		metagranite-granodiorite
KFM01A	241.90	242.10	X		meta-granodiorite
KFM01A	242.25	242.55		X	meta-granodiorite
KFM01A	315.85	316.25		X	metagranite-granodiorite
KFM01A	317.80	318.00	X		metagranite-granodiorite
KFM01A	355.10	355.30	X		amphibolite
KFM01A	355.30	355.50		X	amphibolite
KFM01A	432.96	433.15		X	amphibolite
(No corresponding petrophysical sample)					
KFM01A	473.53	473.71		X	amphibolite
KFM01A	474.00	474.20	X		amphibolite
KFM01A	476.60	476.80	X		metagranite-granodiorite
KFM01A	477.10	477.50		X	metagranite-granodiorite
KFM01A	521.10	521.40		X	metagranodiorite-tonalite
KFM01A	521.40	521.60	X		metagranodiorite-tonalite
KFM01A	704.69	705.10		X	metagranite-granodiorite
KFM01A	706.00	706.20	X		metagranite-granodiorite
KFM01A	947.40	947.80		X	metagranite-granodiorite
KFM01A	947.80	948.00	X		metagranite-granodiorite
KFM01A	969.90	970.10	X		metagranite
KFM01A	970.10	970.50		X	metagranite

Table 3-3. Petrophysical samples and samples for gamma-ray spectrometry from drillhole KFM02A.

Drillhole ID	Sec up (m)	Sec low (m)	Petro-physical sample	Gamma-ray spectrometry sample	Rock type
KFM02A	244.40	244.60	X		metagranite-granodiorite
KFM02A	245.55	245.75		X	metagranite-granodiorite
KFM02A	263.15	263.35	X		episyenite
KFM02A	263.35	263.68		X	episyenite
KFM02A	277.29	277.60		X	episyenite
KFM02A	277.90	278.10	X		episyenite
KFM02A	295.45	295.64	X		episyenite
KFM02A	295.64	295.81		X	episyenite
KFM02A	316.63	316.83	X		metagranite-granodiorite
KFM02A	316.85	317.05		X	metagranite-granodiorite
KFM02A	317.05	317.45		X	metagranite-granodiorite
KFM02A	317.45	317.65	X		metagranite-granodiorite
KFM02A	350.60	350.80	X		metagranite-granodiorite
KFM02A	350.80	351.00		X	metagranite-granodiorite
KFM02A	351.00	351.20	X		metagranite-granodiorite
KFM02A	351.45	351.85		X	metagranite-granodiorite
KFM02A	552.43	552.63	X		metagranite
KFM02A	552.66	552.86		X	metagranite
KFM02A	712.05	712.25			metagranite-granodiorite
KFM02A	712.25	712.45	X		metagranite-granodiorite
KFM02A	915.90	916.10	X		metatonalite
KFM02A	916.85	917.05		X	metatonalite
KFM02A	949.67	949.87	X		metagranite-granodiorite
KFM02A	949.90	950.10		X	metagranite-granodiorite
KFM02A	953.25	953.45		X	metagranite-granodiorite
KFM02A	953.48	953.68	X		metagranite-granodiorite

Table 3-4. Petrophysical samples and samples for gamma-ray spectrometry from drillhole KFM03A and KFM03B.

Drillhole ID	Sec up (m)	Sec low (m)	Petrop-hysical sample	Gamma-ray spectrometry sample	Rock type
KFM03B	60.46	60.66	X		pegmatitic granite
KFM03B	62.09	62.28		X	pegmatitic granite
KFM03A	157.00	157.20	X		leucogranite
KFM03A	157.20	157.40		X	leucogranite
KFM03A	165.50	165.70	X		metagranite-granodiorite
KFM03A	165.70	165.90		X	metagranite-granodiorite
KFM03A	239.44	239.64	X		metatonalite
KFM03A	239.64	239.84		X	metatonalite
KFM03A	310.49	310.75	X		metatonalite
KFM03A	310.75	310.96		X	metatonalite
KFM03A	432.75	432.95	X		metagranite-granodiorite
KFM03A	433.07	433.27		X	metagranite-granodiorite
KFM03A	504.00	504.20	X		metagranite-granodiorite
KFM03A	504.20	504.40		X	metagranite-granodiorite
KFM03A	620.00	620.20		X	metagranite-granodiorite
KFM03A	619.80	620.00	X		metagranite-granodiorite
KFM03A	856.82	857.02	X		metagranite-granodiorite
KFM03A	860.32	860.52		X	metagranite-granodiorite
KFM03A	957.20	957.40	X		metagranite-granodiorite
KFM03A	957.40	957.60		X	metagranite-granodiorite

4 Density and magnetic properties

Different rock types vary in composition and this leads to variations in their petrophysical properties. The rock density and magnetic properties (susceptibility and remanence) are therefore often used as supportive information when classifying rocks. These properties are important for the interpretation of geophysical data and they also constitute input parameters when modelling gravity and magnetic data.

4.1 Data processing

In order to get a better picture of the data and to increase the possibility to compare different data sets and data from different rock types, a number of sub-parameters are often calculated from the density, the magnetic susceptibility and the magnetic remanence. Two such sub-parameters are the silicate density and the Q-value (Königsberger ratio). The silicate density /3/ provides an estimation of the rock composition and is calculated by correcting the measured total density for the content of ferromagnetic minerals (e.g. magnetite and pyrrhotite) by use of the magnetic susceptibility. The Q-value /4/ is the quotient between the remanent and induced magnetization:

$$Q = \frac{M_R}{M_I} = \frac{M_R}{KH} = \frac{M_R \mu_0}{KB}$$

where

M_R = Remanent magnetization intensity (A/m),

M_I = Induced magnetization (A/m),

K = Magnetic susceptibility (SI),

H = Magnetic field strength (A/m),

B = Magnetic flux density (T),

μ_0 = Magnetic permeability in vacuum ($4\pi\ 10^{-7}$ Vs/Am).

The Q-value thus indicates the contribution of the remanent magnetization to the measured anomalous magnetic flux density and is therefore an important parameter when interpreting and modelling ground and airborne magnetic data. The Q-value is also grain size dependent and indicates what ferromagnetic minerals that is present in the rock.

In this investigation the so called density-susceptibility rock classification diagrams (see for example Figure 4-1) were used. The ordinate axes in these diagrams display the magnetic susceptibility on the left hand side and the estimated magnetite content to the right. It has been shown that in rocks in which the magnetic susceptibility is primarily governed by magnetite, there is a fairly good correlation between the magnetic susceptibility and the magnetite content /5/. However, the scatter is fairly high so predictions of the volume-per-cent magnetite in rocks based on the magnetic susceptibility should be used with caution. The silicate density curves are based on equations from Henkel 1991 /3/, and the average densities of each rock type originate from Puranen 1989 /6/. The diagram should be read in the way that if a rock sample plots on, or close to, a “rock type curve” it is indicated that the rock should be classified according to the composition of this rock type. Since there is often a partial overlap of the density distributions of different rock types, there is always a certain degree of uncertainty in the classification. A sample plotting in between, for example, the granite and granodiorite curves should thus be classified as granite to granodiorite.

4.2 Results KFM01A

Four of the metagranite to granodiorite samples cluster tightly close to the granite curve in the density-susceptibility rock classification diagrams in Figure 4-1. Their average density is 2,661 ± 2 kg/m^3. The outlying sample (depth c 476 m) has a significantly lower magnetic susceptibility but a slightly higher density than the other samples of this group. The two amphibolites have a fairly low magnetic susceptibility, which is normal for this rock type, and densities of 2,989 kg/m^3 and 3,048 kg/m^3. One group C metagranite sample has a density of 2,642 kg/m^3, the lowest value of all samples in the borehole, whereas the two other samples have densities that indicate a mineral composition corresponding to granodiorite.

The low susceptibility metagranite to granodiorite sample at depth c 476 m also have a lower remanent magnetization intensity then the other samples of the group, but its Q-value of 1.01 is slightly higher than the group average (Figure 4-2). The two amphibolite samples have very low Q-values (average of Q = 0.002) and the three group C samples have Q-values in the same range as the metagranite to granodiorite samples of group B8. The inclination of the NRM vector is generally fairly steep (50–70°), which is normal for these rock types (Figure 4-3). Two samples have negative inclinations, one amphibolite and one group C metagranite, and this may indicate that these rocks could have suffered from e.g. thermal alteration.

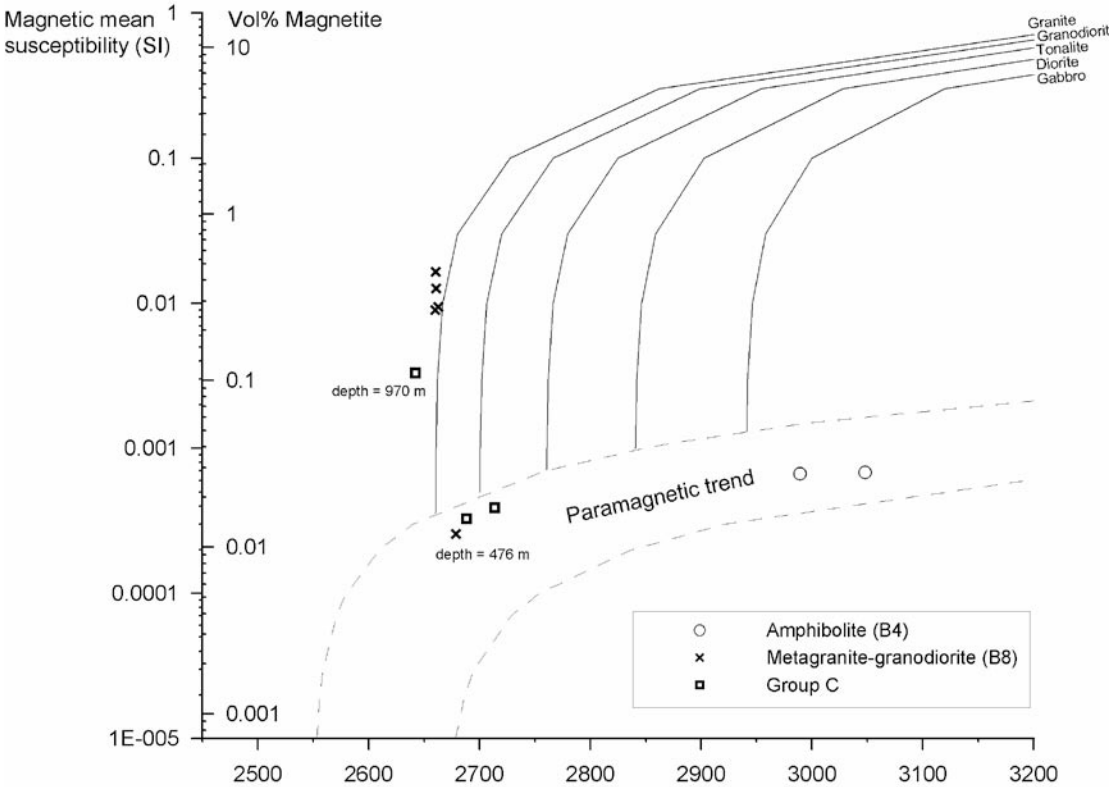

Figure 4-1. *Density-susceptibility rock classification diagram for the rocks of KFM01A. See text for explanation.*

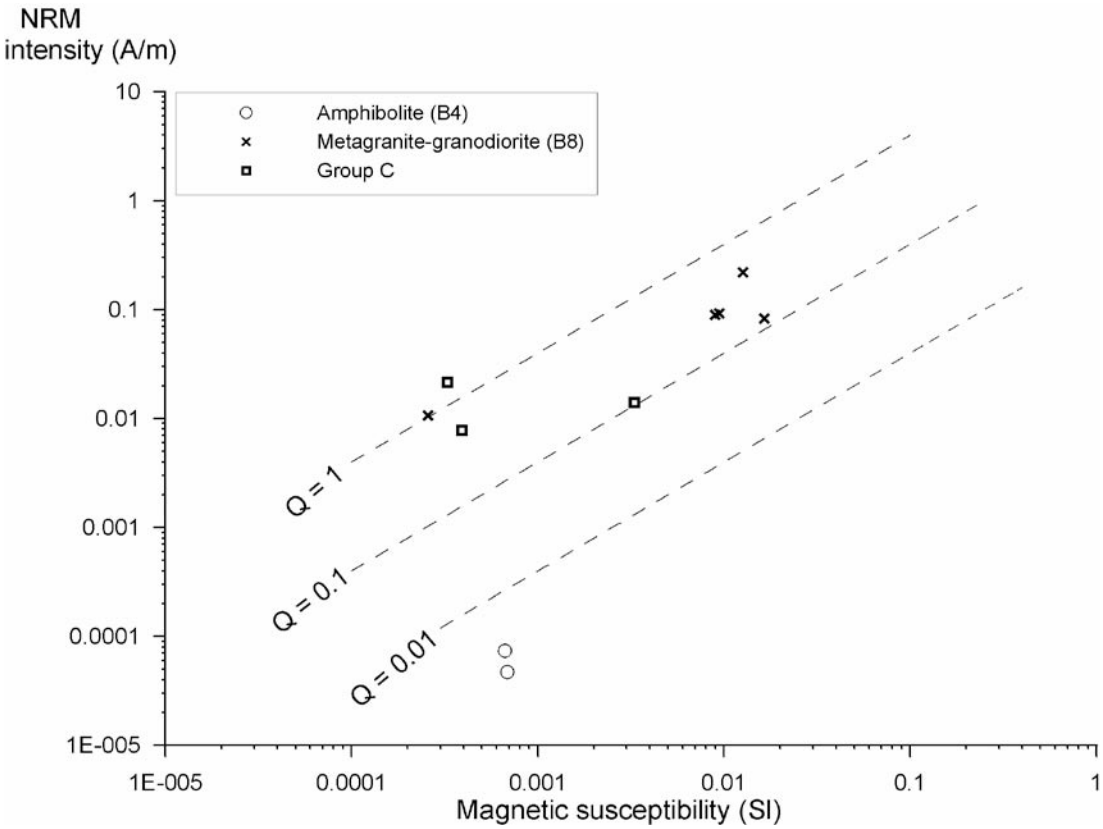

Figure 4-2. *NRM intensity versus magnetic susceptibility for the rock samples of KFM01A. Hatched lines indicate Q-values of 0.01, 0.1 and 1. See text for explanation.*

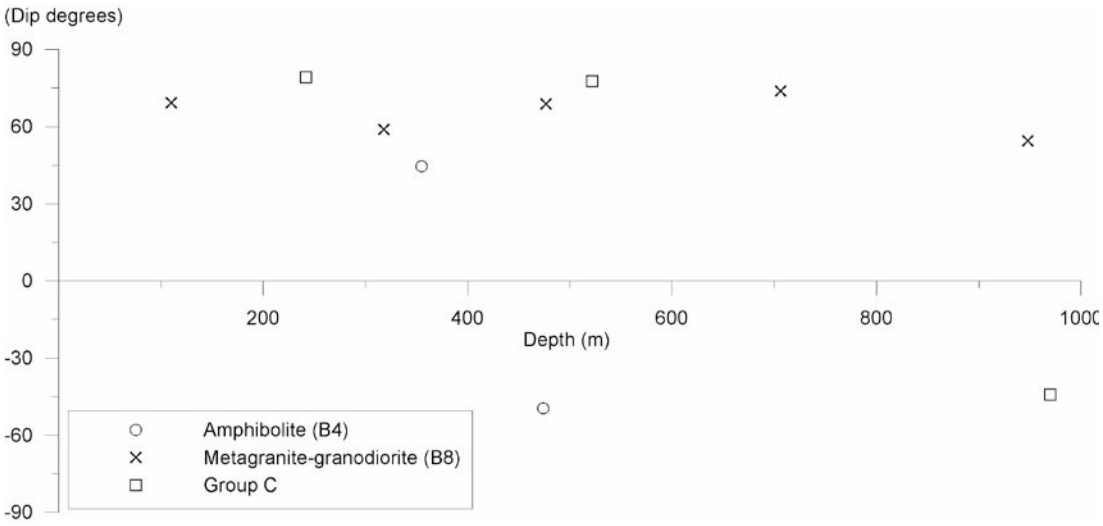

Figure 4-3. *Inclination (mean of 4 specimens) of the NRM vector versus depth for KFM01A. See text for explanation.*

4.3 Results KFM02A

The metagranite to granodiorite (B8) and metagranite (B9) samples have a narrow density distribution with an average of 2,651 ± 6 kg/m^3 (Figure 4-4). Two samples (depth 244 m and 712 m) have significantly lower magnetic susceptibilities than the rest of the group. The group C metatonalite (depth 916 m) has a density that indicates a mineral composition corresponding to diorite rock, whereas the group C metagranite has a density well in accordance with the group B8 and B9 rock samples. The porous rocks have very low densities, ranging from 2,064 kg/m^3 to 2,568 kg/m^3, and also very low magnetic susceptibilities averaging at c 0.0002 SI.

The porous rock samples have Q-values of 0.57, 1.24 and 2.06 (Figure 4-5). A Q-value of 2.06 is fairly high, but the effect on the total magnetic flux density distribution is most likely limited due to the low remanent magnetization intensity of 0.026 A/m of the rock. The group B8 and B9 rocks have Q-values between 0.13 and 0.58. Note that the two low-susceptibility samples (depth 244 m and 712 m) also have a low remanence intensity, which clearly indicates that these rock samples have a significantly lower content of magnetite than the other samples of this group. The inclination of the NRM vector is generally fairly steep (50–70°), which is normal for these rock types (Figure 4-6). Two samples have shallow NRM inclinations and the porous metagranitoid sample shows a negative inclination, which is possibly related to the alteration of this rock.

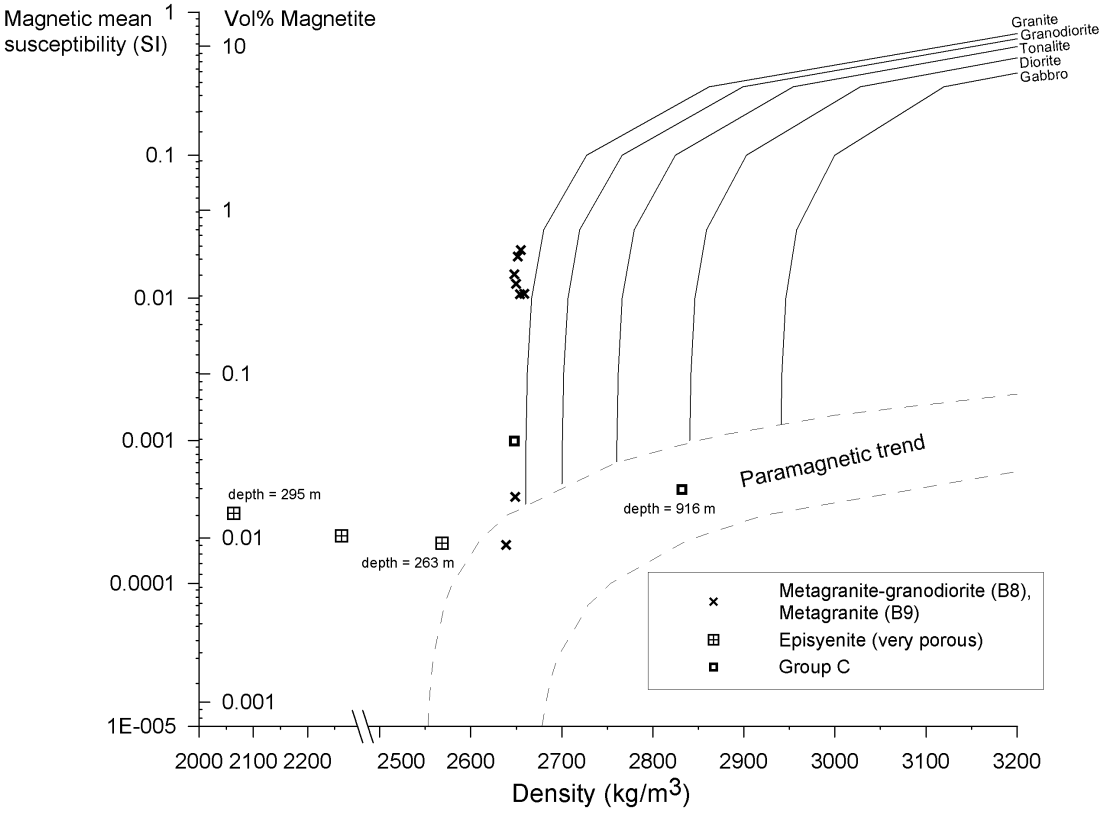

Figure 4-4. *Density-susceptibility rock classification diagram for the rocks of KFM02A. See text for explanation.*

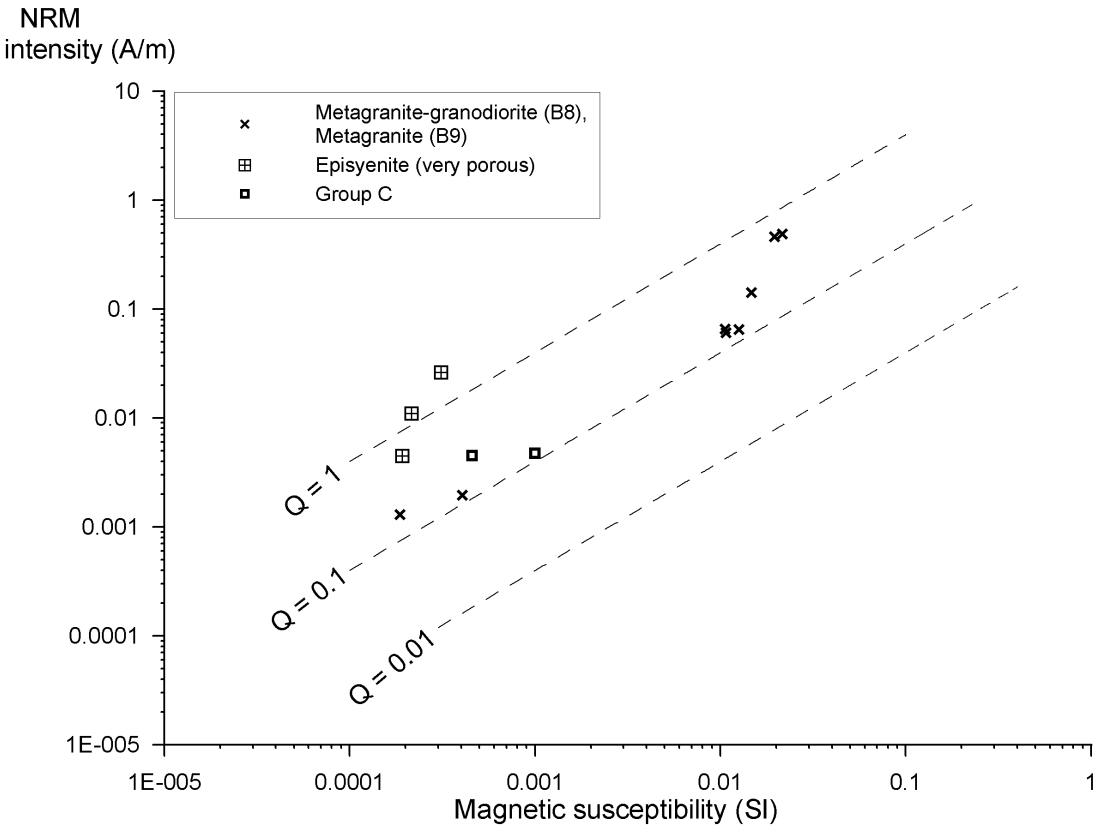

Figure 4-5. *NRM intensity versus magnetic susceptibility for the rock samples of KFM02A. Hatched lines indicate Q-values of 0.01, 0.1 and 1. See text for explanation.*

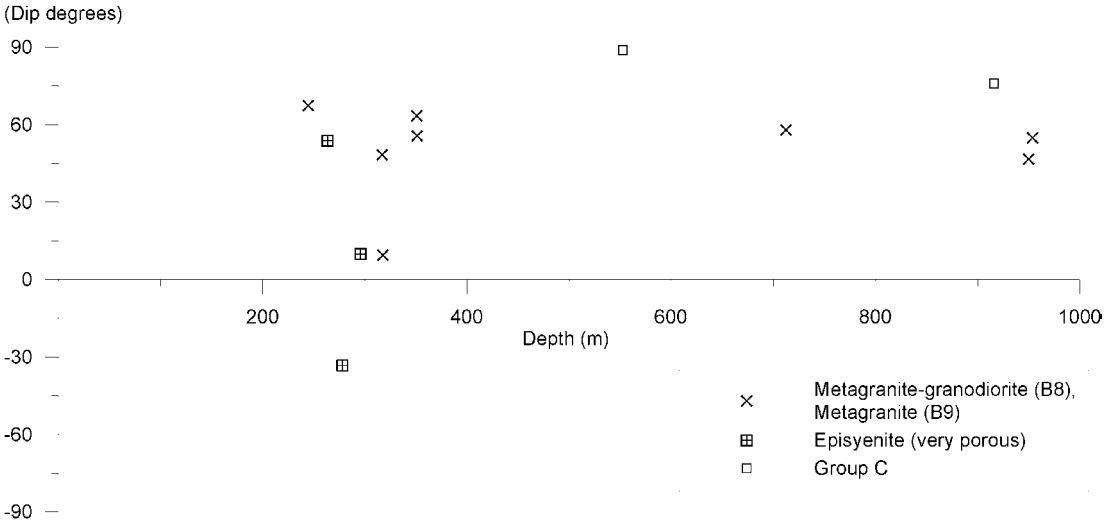

Figure 4-6. *Inclination (mean of 4 specimens) of the NRM vector versus depth for KFM02A. See text for explanation.*

4.4 Results KFM03A and KFM03B

Five of the metagranite to granodiorite samples cluster tightly close to the granite curve in the density-susceptibility rock classification diagrams in Figure 4-7. The outlying sample (depth c 619 m) has a significantly lower magnetic susceptibility but the density corresponds well to the rest of the group. The average density of all six samples is 2,653 ± 2 kg/m^3. The two metatonalite samples (group B5 and group C) plot between the tonalite and diorite rock type curves, thus indicating a mineral composition that corresponds to tonalite to diorite rock. The metagranite of group D has a low density of 2,627 kg/m^3 and the pegmatitic granite of KFM03B is only slightly denser but has a significantly lower content of magnetic minerals.

The anomalous metagranite to granodiorite sample (depth c 619 m) has a relatively high Q-value of 1.41 whereas the other group B8 samples and the metatonalite (group C) have Q-values between 0.1 and 1.0 (Figure 4-8). The rest of the samples have Q-values below 0.2. The inclination of the NRM vector is rather shallow throughout the entire borehole, varying between c 10–40° (Figure 4-9). This is anomalous compared to the data from KFM01A, KFM02A and from the surface data /1/.

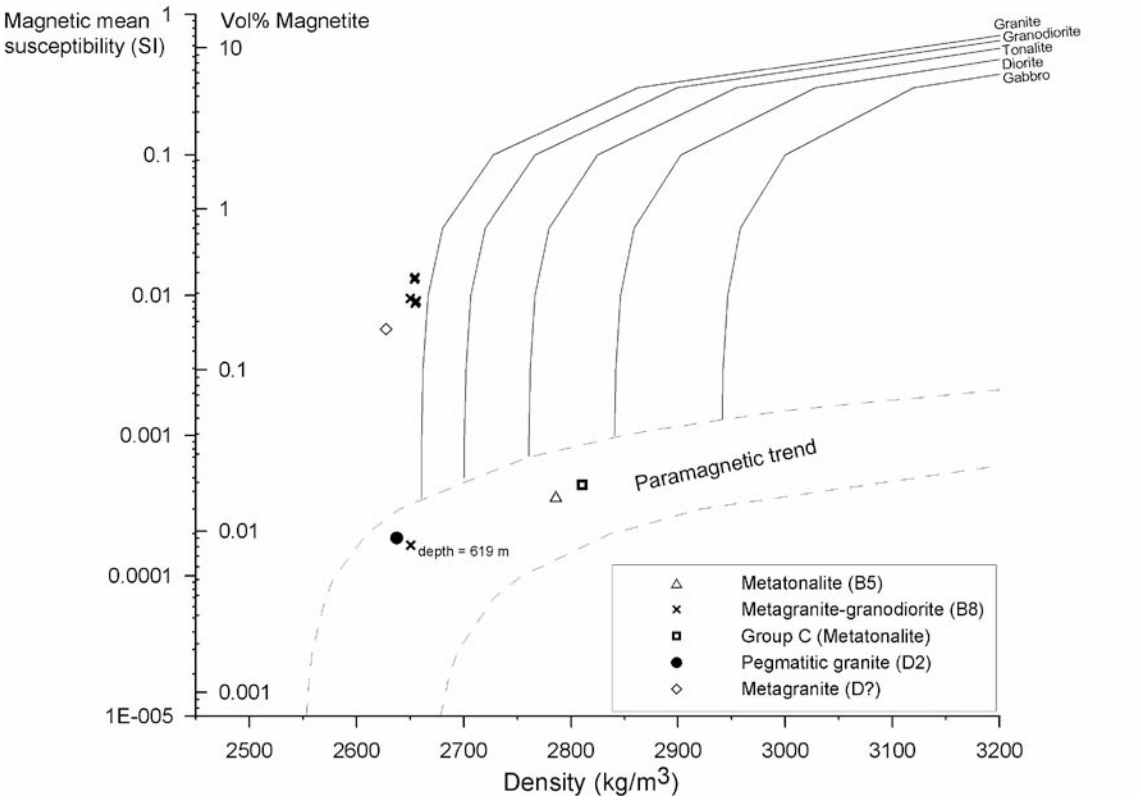

Figure 4-7. *Density-susceptibility rock classification diagram for the rocks of KFM03A and KFM03B. See text for explanation.*

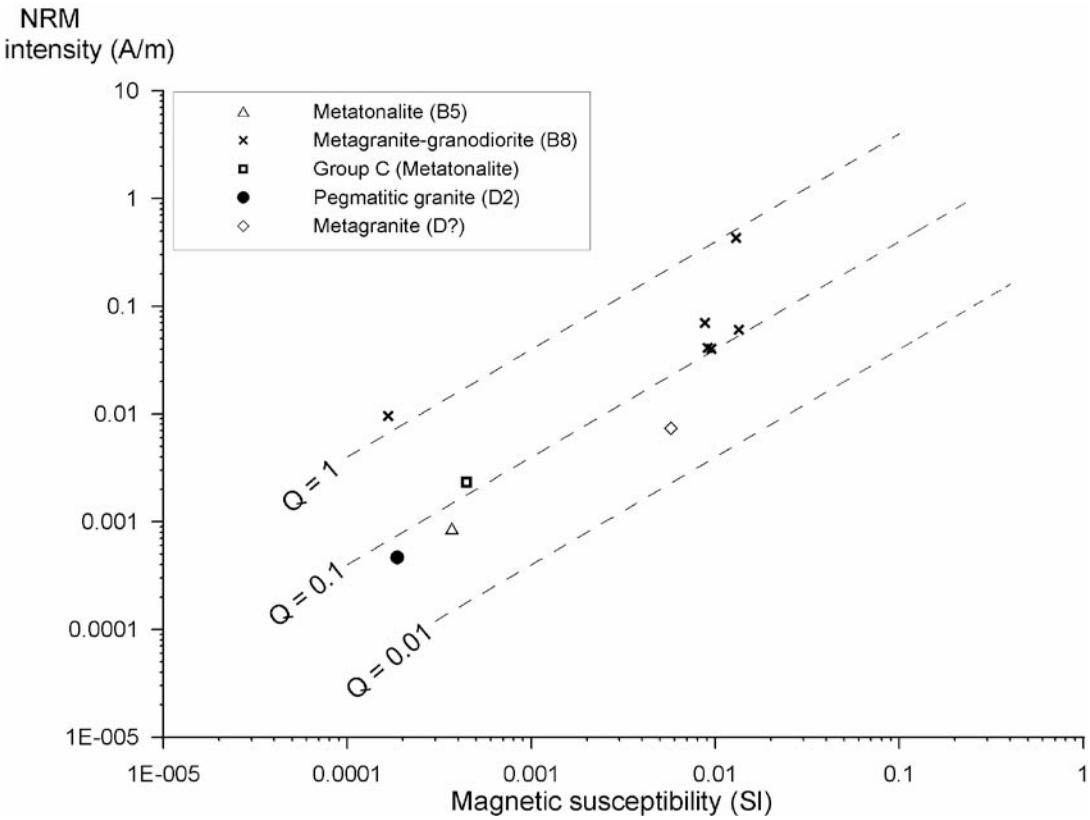

Figure 4-8. *NRM intensity versus magnetic susceptibility for the rock samples of KFM03A and KFM03B. Hatched lines indicate Q-values of 0.01, 0.1 and 1. See text for explanation.*

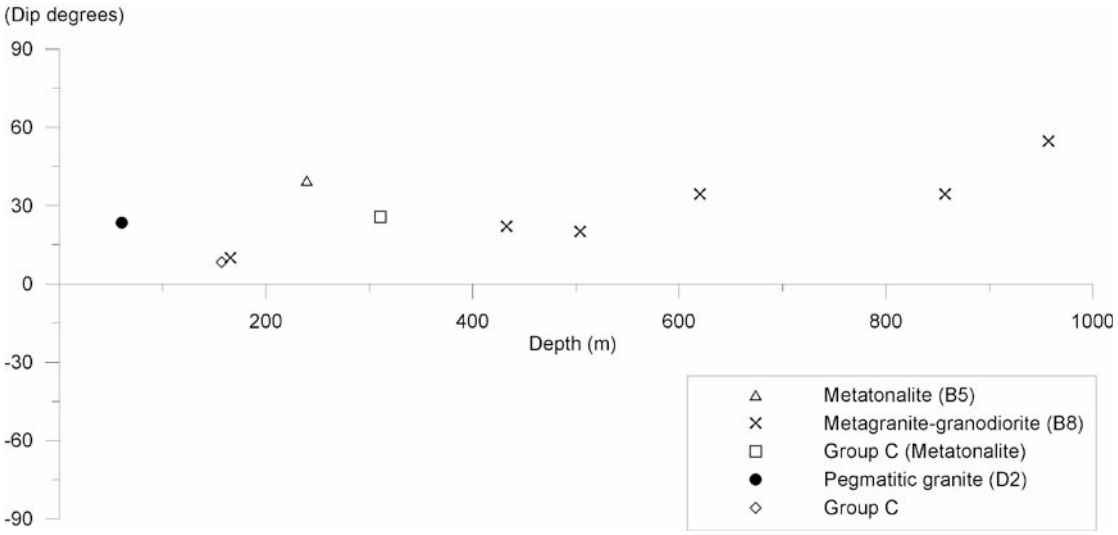

Figure 4-9. *Inclination (1 specimen) of the NRM vector versus depth for KFM03A and KFM03B. See text for explanation.*

5 Anisotropy of magnetic susceptibility (AMS)

The magnetic anisotropy of rock forming minerals basically originates from two sources, the grain shape and the crystallographic structure. The orientation of the anisotropy of magnetic susceptibility coincides with the crystallographic axes for most rock forming minerals, and it is therefore possible to directly transfer "magnetic directions" to "tectonic directions" (foliation and lineation) measured in the field. Since magnetite carries a very high magnetic susceptibility in comparison to most other rock forming minerals, even a low grade tends to dominate the magnetic properties, including the anisotropy of a rock.

For further descriptions of the method, see e.g. /7/ or /8/.

5.1 Data processing

The four measurements on individual specimens allow a calculation of mean directions of the principal AMS axes (called the sample mean direction) and corresponding "sample mean value" of the degree of anisotropy (P), degree of lineation (L), degree of foliation (F) and ellipsoid shape (T). When calculating the sample mean values of the P, L, F and T parameters, the orientations of the ellipsoids of each specimen are taken into account. Vector addition is applied to the three susceptibility axes of the four specimens from the sample, which results in a "sample mean ellipsoid". The sample mean values of the anisotropy parameters thus give information of the sample as a whole and are not just "simple" average values. According to statistical demands at least six measurements (specimens) are required for estimating uncertainty regions of the calculated mean directions. No such calculations were therefore performed. Instead, the data quality of each sample was evaluated by visual inspection and sample mean directions based on scattered specimen directions were rejected. For two samples, only two specimens were measured. The corresponding principal axes fell close to each other and the mean direction was accepted as a sample mean direction.

5.2 Results KFM01A

The degree of magnetic anisotropy is moderate to high for a majority of the samples (Figure 5-1a). There is a tendency of a correlation between the degree of the anisotropy and the magnetic susceptibility, which indicates that the degree of anisotropy can not be used as an indication of the degree of tectonic strain. The shape of the anisotropy ellipsoid (Figure 5-1b) indicates dominant S-tectonites in the uppermost 600 m of the borehole ($T > 0$). There is a tendency (with respect to the few data points) that the metagranite to granodiorite rock fabric changes in shape with depth, going from dominant S-tectonite to dominant L-tectonite ($T < 0$). This may indicate a depth dependent variation of the type of deformation of the rocks in the vicinity of the borehole. The magnetic foliation planes dip steeply throughout the entire borehole (Figure 5-1c) whereas the magnetic lineations mainly dip moderately (Figure 5-1d).

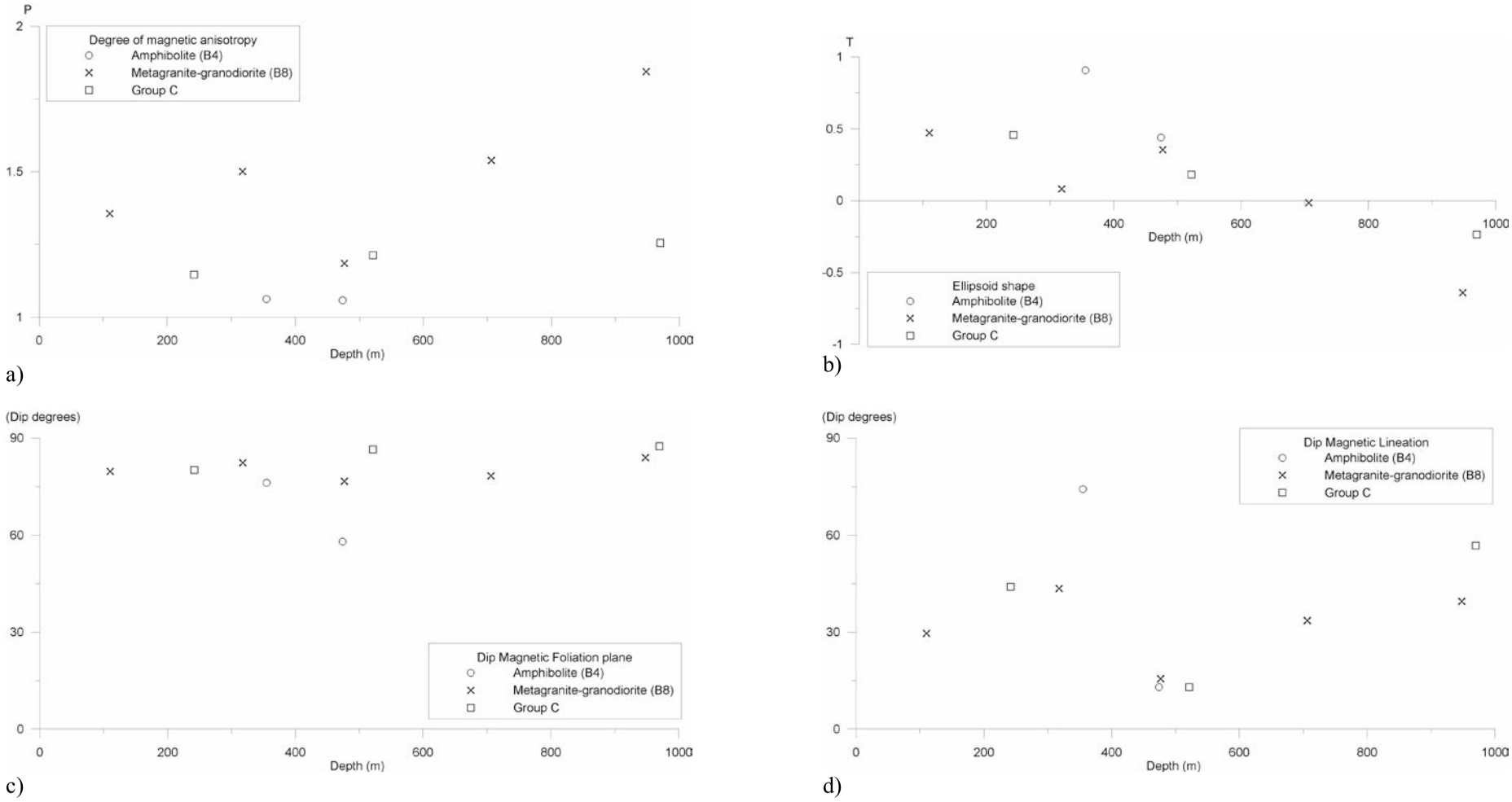

Figure 5-1. *Mean anisotropy parameters plotted with reference to the borehole depth of KFM01A. a) The degree of magnetic anisotropy. b) The shape of the anisotropy ellipsoid. c) The dip of the magnetic foliation plane. d) The dip of the magnetic lineation.*

5.3 Results KFM02A

The degree of magnetic anisotropy is mainly moderate, but low for the altered samples (Figure 5-2a). There is a clear correlation between the degree of the anisotropy and the magnetic susceptibility, which indicates that the degree of anisotropy can not be used as an indication of the degree of tectonic strain. The shape of the anisotropy ellipsoid (Figure 5-2b) indicates dominant L-tectonites in the uppermost c 400 m of the borehole. There is a tendency (with respect to the few data points) of a change in shape with depth, moving towards a neutral ellipsoid in the deeper parts of the borehole. The magnetic foliation planes dip moderate close to the altered section at about 300 m depth, and show mainly steep dips in the rest of the borehole (Figure 5-2c). The dip of the magnetic lineation is moderate throughout the entire borehole (Figure 5-2d).

5.4 Results KFM03A and KFM03B

The degree of magnetic anisotropy is low to moderate for a majority of the samples (Figure 5-3a). There is only a weak tendency of a correlation between the degree of the anisotropy and the magnetic susceptibility, which indicates that the degree of anisotropy may be used as an indication of variations of the degree of tectonic strain. The shape of the anisotropy ellipsoid (Figure 5-3b) indicates dominant weak S-tectonites throughout the entire borehole. The magnetic foliation planes mainly show shallow to moderate dips (Figure 5-3c), and it is the same also for the dip of the magnetic lineation (Figure 5-3d). These shallow dips are anomalous in comparison to the other two boreholes and also to the surface data.

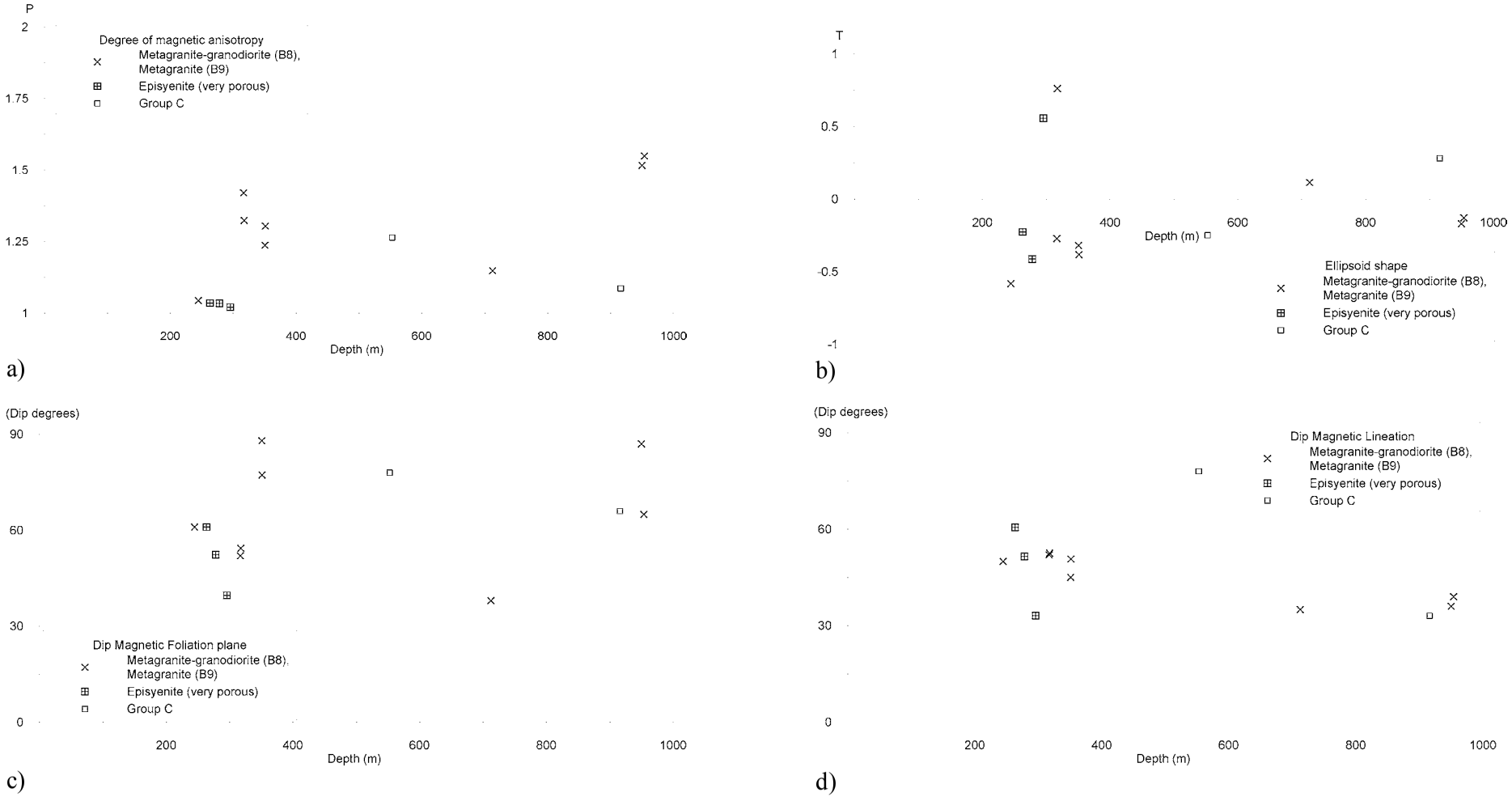

Figure 5-2. *Mean anisotropy parameters plotted with reference to the borehole depth of KFM02A. a) The degree of magnetic anisotropy. b) The shape of the anisotropy ellipsoid. c) The dip of the magnetic foliation plane. d) The dip of the magnetic lineation.*

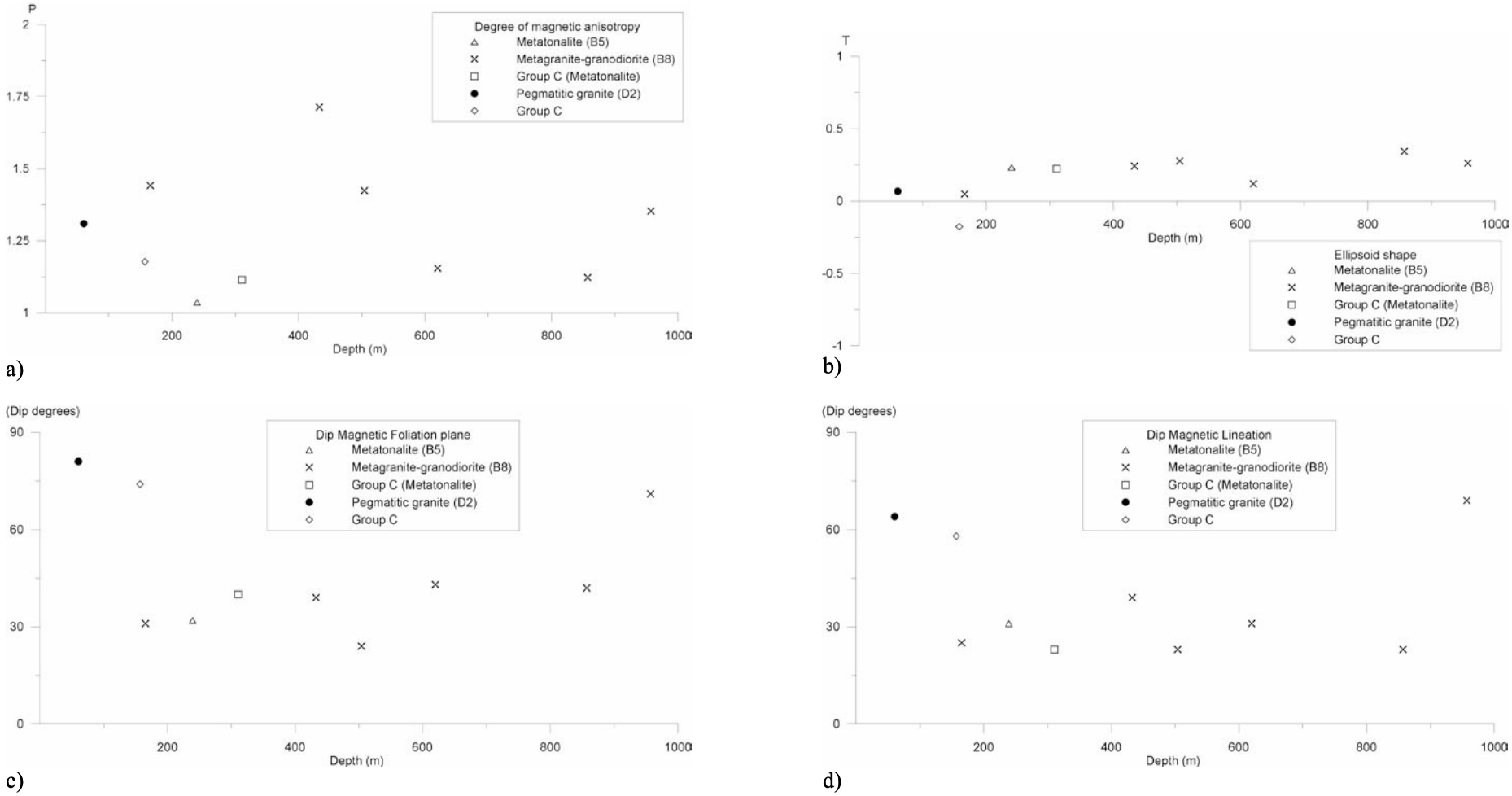

Figure 5-3. *Mean anisotropy parameters plotted with reference to the borehole depth of KFM03A and KFM03B. a) The degree of magnetic anisotropy. b) The shape of the anisotropy ellipsoid. c) The dip of the magnetic foliation plane. d) The dip of the magnetic lineation.*

6 Electrical properties and porosity

Electric resistivity

The contrast in resistivity (ρ) between silicate minerals and more conducting media like water or sulphides/graphite is extremely high. The bulk resistivity of a rock is therefore more or less independent of the type of silicate minerals that it contains. Electric conduction will be almost purely electrolytic if the rock is not mineralised. Archie's law /9/ is frequently used to calculate the conductivity (1/ρ) of sedimentary rocks.

$$\sigma = a \cdot \sigma_w \cdot \varphi^m \cdot s^n$$

where

σ = bulk conductivity (= 1/ρ, S/m),

σ_w = pore water conductivity (S/m),

φ = volume fraction of pore space,

s = fraction of pore space that is water saturated,

a, m, n = dimensionless numbers, m ≈ 1.5 to 2.2.

Archie's law has proved to work well for rocks with a porosity of a few percent or more. Old crystalline rocks usually have a porosity of 0.1 to 2% and sometimes even less. With such low porosity the interaction between the electrolyte and the solid minerals becomes relevant. Some solids, especially clay minerals, have a capacity to adsorb ions and retain them in an exchangeable state /10/. This property makes clays electrically conductive but the same property can to some degree be found for most minerals. The resulting effect, surface conductivity, can be accounted for by the parameter a in Archie's law. The relative effect of surface conductivity will be greatly reduced if the pore water is salt. The amount of surface conductivity is dependent upon the grain size and texture of the rock. Fine grained and/or mica- or chlorite-rich, foliated rocks are expected to have a large relative portion of thin membrane pore spaces that contribute to surface conductivity.

The electric resistivity is in reality not a simple scalar. Most rocks show electric anisotropy and the resistivity is thus a tensor. On a micro-scale the anisotropy is caused by a preferred direction of pore spaces and micro fractures.

Induced polarisation

The IP effect can be caused by different mechanisms of which two are the most important. When the electric current passes through an interface between electronic and electrolytic conduction there is an accumulation of charges at the interface due to the kinetics of the electrochemical processes involved. This will occur at the surface of sulphide, oxide or graphite grains in a rock matrix with water filled pores. The second mechanism is related to electric conduction through thin membrane pore spaces. In this case an accumulation of charges will occur at the beginning and end of the membrane. The membrane polarisation is thus closely related to the surface conduction effect mentioned above for electric resistivity. Fine grained and/or mica- or chlorite-rich, foliated rocks are therefore expected to show membrane polarisation. Also, the effect of membrane polarisation is greatly reduced in salt water in the same way as surface conductivity.

6.1 Data processing

A correction for drift caused by drying of the sample during measurements is done automatically by the instrumentation software by comparing the harmonics of low frequency measurements with the base frequency result of the next higher frequency.

The resistivity data were compared with the measured porosity in order to make a fit in accordance to Archie's law.

Apparent values of *m* in Archie's law can be estimated from measurements of resistivity in salt water since the relative effect of surface conductivity becomes small there. High values will be indicative for samples with a large portion of vugs, constrictions and crocked pore paths. Low values will indicate fairly straight pore paths with small variations in cross-sectional area. Using the known values of σ, σ_w and φ, an apparent value of the parameter *a* was calculated for measurements in fresh water. High values will correspond to a large contribution from surface conductivity and vice versa.

6.2 Results

The electrical properties show no significant differences between the three boreholes. The IP data in salt water from KFM03 were suspicious and the samples were therefore re-measured with an intermediate drying and soaking. The data quality was however not improved and no results regarding IP in salt water are presented for the KFM03 samples.

Porosity

The porosity of the majority of the samples cluster in a fairly tight interval between 0.25 and 0.75%. An exception is the samples of vuggy granite/episyenite that show porosities of more than 1% including one sample exceeding 10%. The porosity of the KFM03 samples is slightly higher (median 0.46%) than the KFM01 samples (0.30%) and the KFM02 samples (0.38%, episyenite/vuggy granite excluded). The number of samples of some of the rock groups is quite low but some differences can be noted. The group C and B4 samples have rather low porosities whereas the group D samples have higher porosities.

Electrical properties

The resistivity has been measured with the samples soaked in fresh (~ 42 Ωm) as well as salt (~ 0.29 Ωm) water. I should be noted that the samples were soaked in the water during only a few days and thus full saturation of all pore space might not have been reached. Also, since many of the samples originate from saline environments it is possible that the water in the pores was not in equilibrium with the rest of the soaking water due to dissolution of salts left in the pores.

The resistivity in salt water as a function of porosity can be seen in Figure 6-1. Excluding the episyenite/vuggy granite samples there is no correlation between the two parameters. The effect of surface conductivity is greatly reduced in a saline environment. This implies that the differences in resistivity between the samples to a large extent are due to differences in pore space geometry. If Archie's law is used to model the data and a reasonable value is assumed for the factor *a* it is possible to calculate apparent m-values. The apparent *m*-values range from 1.5 to 2.0 excluding the episyenite/vuggy granite samples. These show significantly larger values indicating presence of e.g. vugs and constrictions in the pore volume.

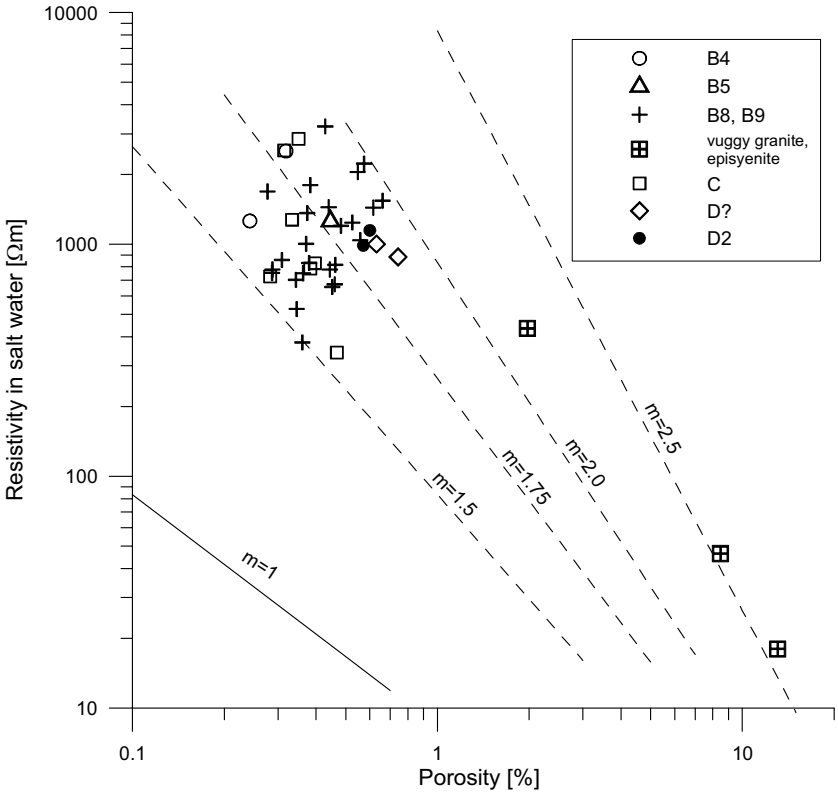

Figure 6-1. *Resistivity in salt water (2.5% NaCl) vs porosity for samples from KFM01A, KFM02A and KFM03A,B. Straight lines corresponding to Archie's law (see text) and a = 3.0 for different values of m are also plotted.*

The resistivity in fresh water as a function of porosity can be seen in Figure 6-2. The vuggy granite/episyenite samples have fairly low resistivity. The resistivity for the other samples are in the interval 4,300 to 55,000 Ωm, which can be regarded as normal values for crystalline rocks. No correlation can be seen between porosity and resistivity. Apparent values for the factor *a* in Archie's law can be calculated using the apparent *m*-values from the salt water measurements. Such apparent *a*-values fall in the interval 25 to 340 (excluding vuggy granite/episyenite samples). The high apparent *a*-values indicate that the resistivity in fresh water is strongly dependent upon surface conductivity. Pore space contact surface is thus of much greater importance than pore space volume. Comparisons with thin-section analysis are not fully conclusive but samples with high apparent *a*-values usually have "locally strongly sericitised plagioclase" and "partly chloritised biotite" and "lenses of prehnite" /2/. Presence of fine grained phyllosilicates thus seems to have a major impact on electrical properties in fresh water. Median apparent *a*-values for type B8 rocks are 56.2 (KFM01A), 92.2 (KFM02A) and 91.6 (KFM03A).

The phase angles (IP effect) measured at 0.1 Hz in fresh water can be seen in Figure 6-3 as a function of resistivity. The IP effect is quite low for all samples. The highest IP values are seen for a D2 sample from KFM03B (62 m depth) and a B8 sample from KFM02A (317 m depth). It can also be noted that the samples with the lowest resistivities (excluding episyenite/vuggy granite samples) also show low IP. This is not surprising since the current might be forced through thin membrane pores in high resistivity samples.

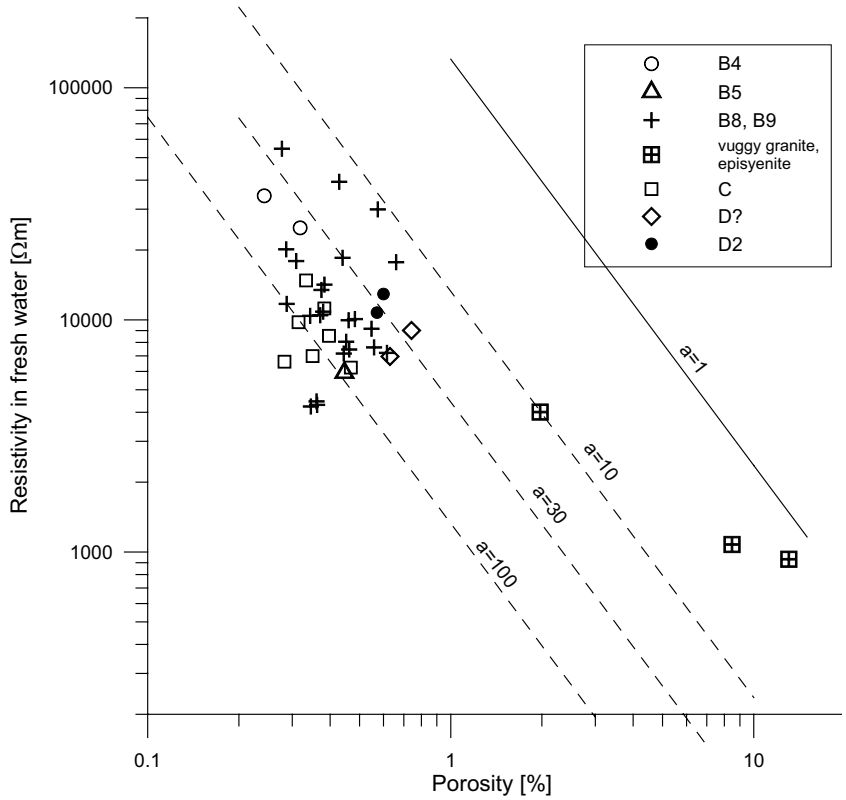

Figure 6-2. *Resistivity in fresh water (42 Ωm) vs porosity for samples from KFM01A, KFM02A and KFM03A,B. Straight lines corresponding to Archie's law (see text) and m = 1.75 for different values of the factor a are also plotted. Note that the choice of m = 1.75 is not valid for some of the samples.*

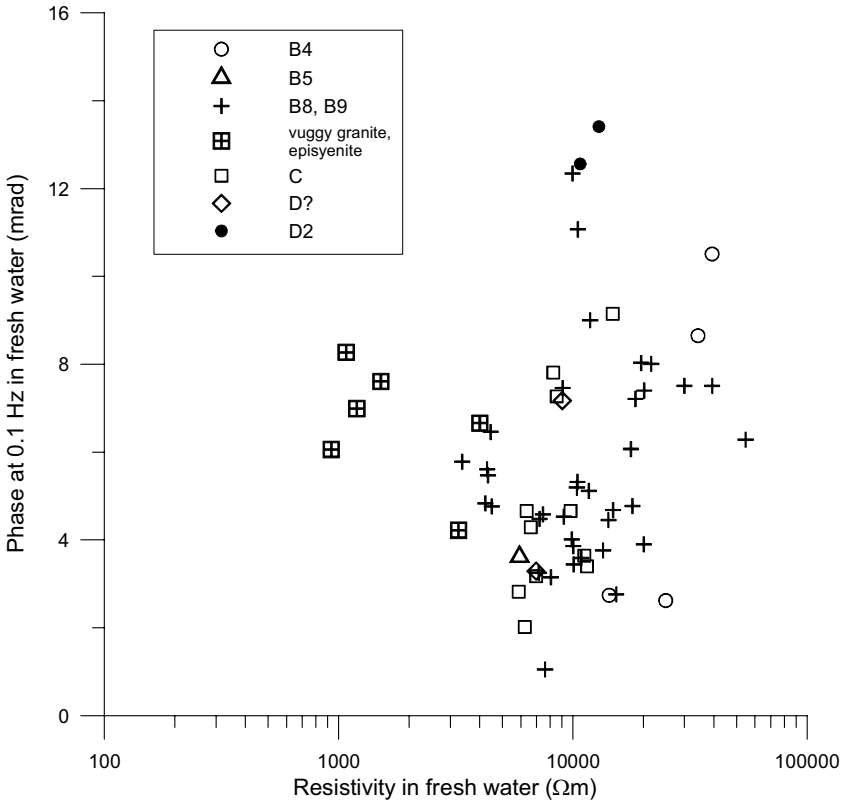

Figure 6-3. *IP effect as phase angle in fresh water (42 Ωm) vs resistivity for samples from KFM01A, KFM02A and KFM03A,B.*

The IP effect as phase angle at 0.1 Hz in fresh and salt water can be seen in Figure 6-4. The samples from KFM03 have been omitted since the IP data in salt water for these samples were of questionable quality. The IP is greatly reduced in salt water indicating that the major cause of the effect is membrane polarisation. Weak residual IP in salt water can be seen for the episyenite/vuggy granite samples. This might be due to presence of haematite. B8 samples from KFM01 at 706 and 947 m depth and from KFM02 at 316 and 317 m depth also show some weak residual IP. These samples are among those with the highest magnetic susceptibilities. The IP effect in salt water might thus be due to magnetite. However, there are other samples with comparable values of magnetic susceptibility that do not show any IP in salt water.

The two parameters m and a from Archie's law are plotted in Figure 6-5. Rocks with a varying degree of alteration might form a trend in such a plot, which has been indicated for rocks sampled in the borehole KSH02 at Simpevarp /11/. A trend with positive correlation between a and m can be seen in Figure 6-5 if episyenite/vuggy granite samples are excluded. The same type of plot can be seen in Figure 6-6 where B8 and B9 rocks from the three boreholes can be compared. The KFM01A samples fall in the lower left of the plot whereas the KFM03A samples group in the upper right with KFM02A samples intermediate. This might be interpreted to be due to a difference in pore space geometry between the different boreholes. In turn, this difference might be caused by an increased amount of alteration minerals like sericite, chlorite and prehnite in KFM03A samples.

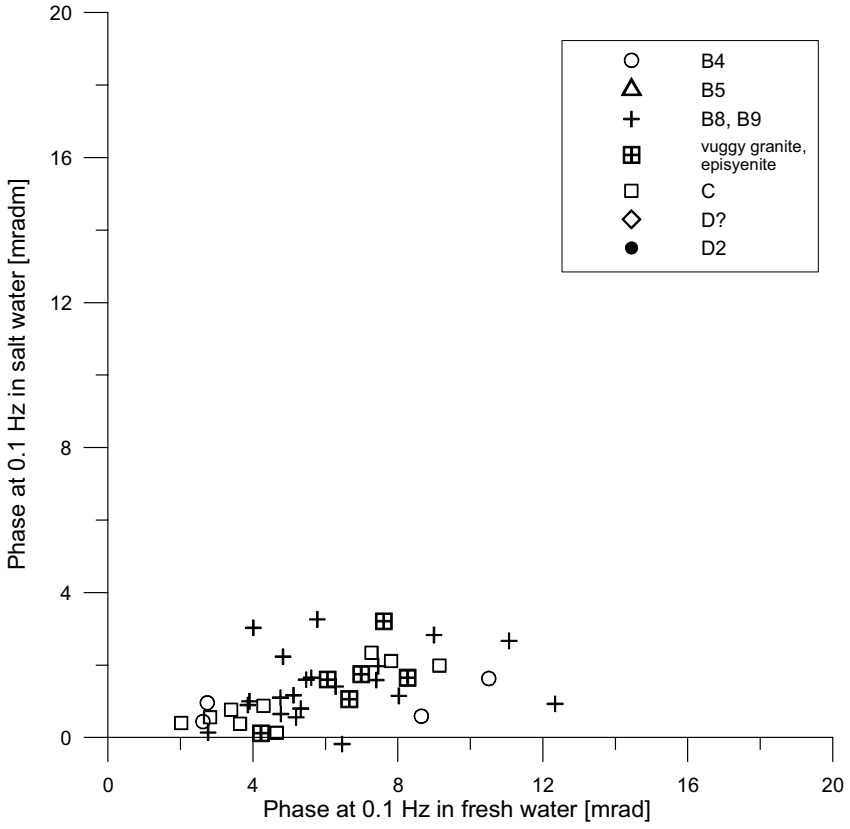

Figure 6-4. *IP effect as phase angle in salt water (0.29 Ωm) vs. IP effect in fresh water (42 Ωm) for samples from KFM01A and KFM02A.*

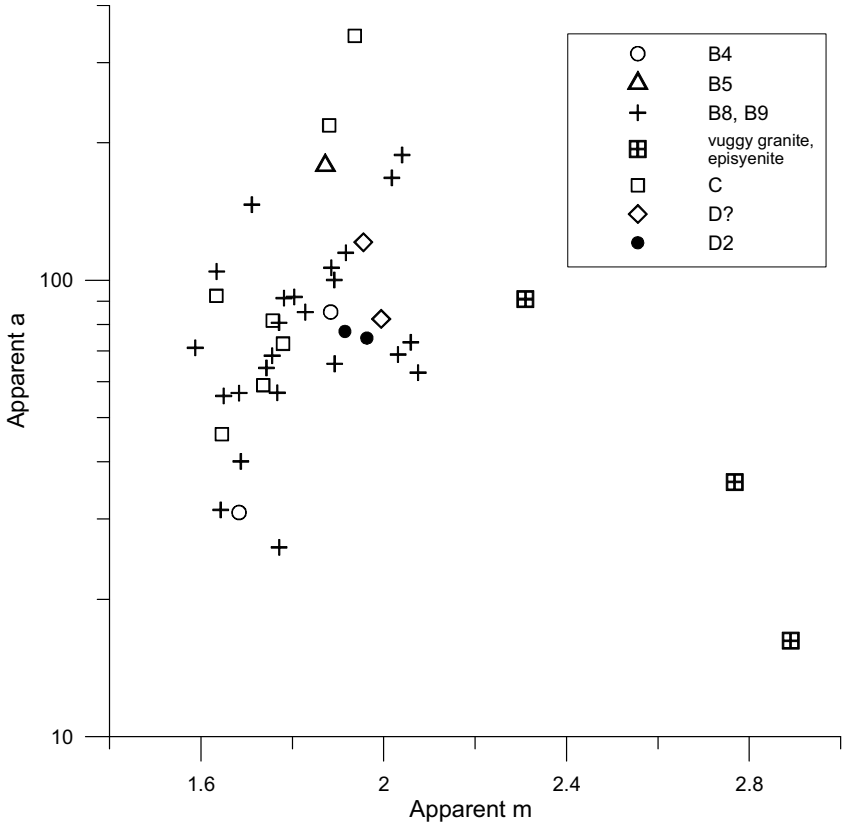

Figure 6-5. *Apparent values of the parameters a and m in Archie's law for samples from KFM01A, KFM02A and KFM03A. See text for explanation.*

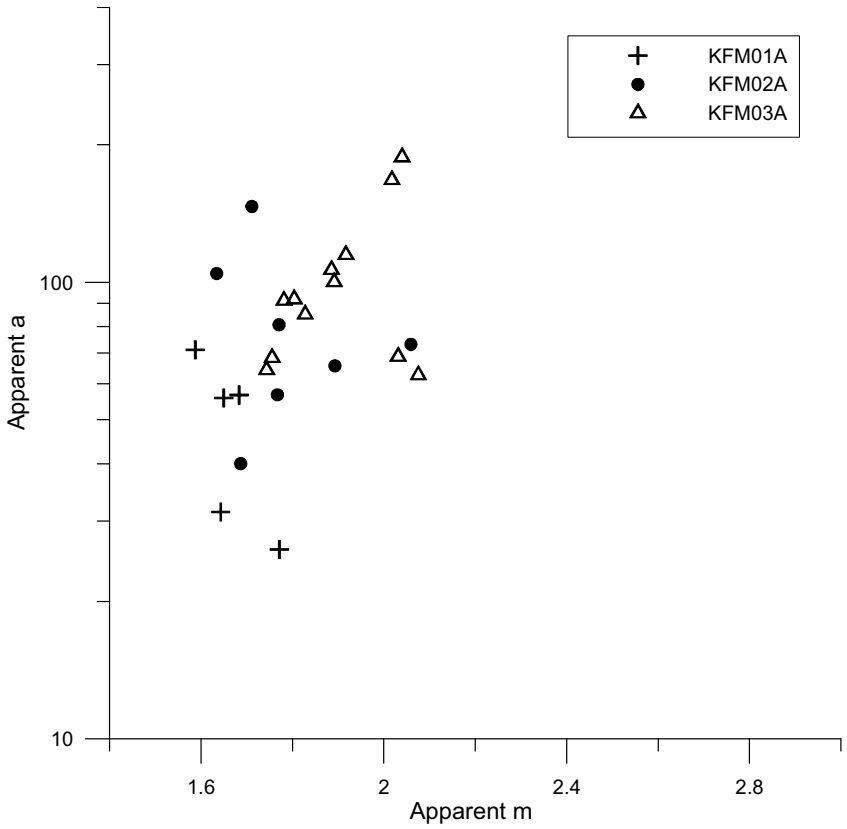

Figure 6-6. *Apparent values of the parameters a and m in Archie's law for rock type B8 and B9 samples from KFM01A, KFM02A and KFM03A. See text for explanation.*

7 Gamma ray spectrometry

The gamma ray spectrometry method is based on the naturally occurring radioactive isotopes of potassium, uranium and thorium, and gives information on the content of these elements. The data is mainly used for bedrock and soil mapping as well as radon investigations.

7.1 Data processing

The data processing has included calculation of e.g. mean values, errors, gamma index and natural exposure rate for each sub-sample and, based on these results, for the main samples.

The gamma index have been calculated according to SIG standards as

$C_K/3{,}000 + C_U/300 + C_{Th}/200$

where C is the concentration of the elements in Bequerel/kg.

The natural exposure rate (μR/h) has been calculated according to /12/ as

1.505*K [%] + 0.625*U [ppm] + 0.310*Th [ppm]

The results of the gamma-ray spectrometry measurements and data processing are presented in Appendix 1 and further analyzed in the following sections.

7.2 Results KFM01A

Results from KFM01A are presented in Figure 7-1, 7-4a and Table 8-1b.

The amphibolite rock (B4) shows gamma ray characteristics common for this rock type, that is, a low potassium, uranium and thorium content, c 1% potassium, 2 ppm uranium and 3 ppm thorium, respectively.

The potassium and uranium content in the metagranite-granodiorite (B8/B9) is within normal levels for granite, 2.3–3.2% and 5–6 ppm respectively. In general, the thorium levels are slightly higher than normal, 15–23 ppm. The thorium dominance compared to typical granite is also reflected in the hue-saturation plot, Figure 7-4a. A sample at 477.3 m shows very low potassium content, 1.2% and a sample at 947.6 m show very low uranium content, 2 ppm.

The rocks within group C are of various compositions. The two metagranodiorite-tonalite and metagranodiorite samples show normal values, 1–2% potassium, 4–5 ppm uranium and 7–17 ppm thorium. A metagranite at 970.3 m shows very high thorium content, 42 ppm, and increased potassium content, 4%, which in total also gives a high natural exposure rate, 23 micro-R/h. These levels are also obtained by chemical analysis /2/. The uranium content is normal, 6 ppm.

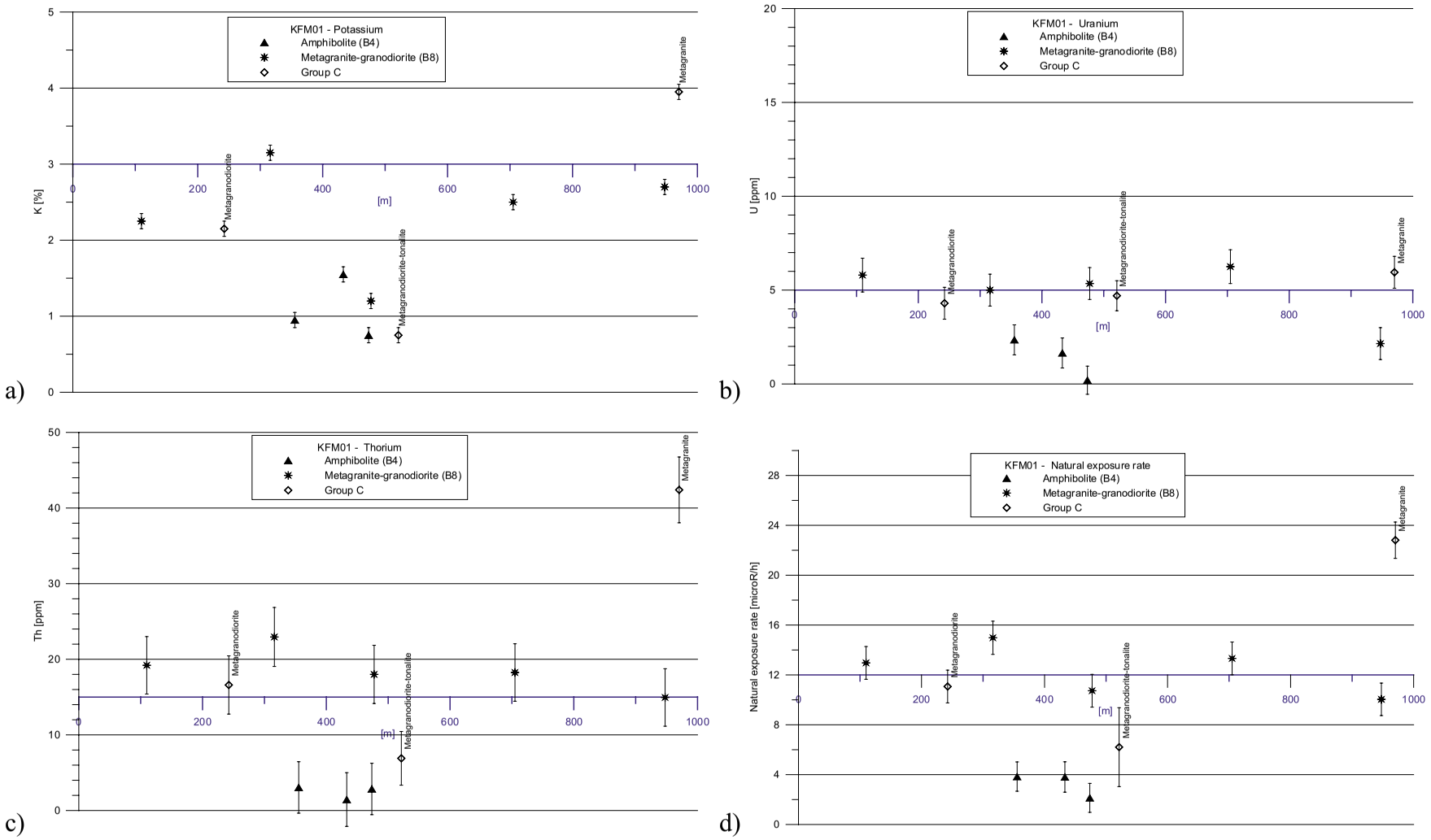

Figure 7-1. *Gamma ray spectrometry data for different rock types, plotted with reference to the borehole depth of KFM01A. a) K content, %. b) U content, ppm. c) Th content, ppm. d) Natural exposure rate, microR/h. Standard error bars are shown. The borehole axis position represents normal levels for granite.*

7.3 Results KFM02A

Results from KFM02A are presented in Figure 7-2, 7-4b and Table 8-2b.

The metagranite-granodiorite (B8/B9) is in general within normal levels for potassium, uranium and thorium, 3–3.5%, 4–8 ppm and 13–17 ppm, respectively. The potassium and thorium enrichment in the sample close to the episyenite samples at 245.65 m (see below) possibly indicate a similar (incipient?) alteration. This sample also shows a low uranium concentration, 2 ppm. A sample at 950.00 m shows a high uranium level, 19 ppm, coincident with very low potassium content, 1.0%.

The episyenite, which is an altered metagranite-granodiorite /13/, shows anomalous levels for both potassium and thorium, 3.4–4.6% K and 19–23 ppm Th, respectively. The uranium level is normal, 4–6 ppm. Hence, the natural exposure rate is higher than normal, 14–18 micro-R/h. Notably is that the most porous samples show the highest relative concentrations, Figure 7-2 a) and d). The potassium-thorium dominance for the episyenite compared to typical granite is also reflected in the hue-saturation plot, Figure 7-4b.

Of the two rock samples within group C, the metagranite at 552.76 m shows high thorium content, 29 ppm, and slight enrichment in uranium and potassium, 8 ppm and 3.6% respectively. The metatonalite shows normal values, 1% potassium, 2 ppm uranium and 10 ppm thorium.

7.4 Results KFM03A and KFM03B

Results from KFM03A and B are presented in Figure 7-3, 7-4c and Table 8-3b.

The metatonalite (B5) sample shows normal values, that is 1.4% potassium, 1 ppm uranium and 11 ppm thorium.

The metagranite-granodiorite (B8/B9) is within normal levels for potassium, uranium and thorium, 2.7–3.5%, 2–6 ppm uranium and 11–20 ppm thorium. However, a generally weak potassium-thorium dominance for most of the metagranite-granodiorite compared to typical granite is reflected in the hue-saturation plot, Figure 7-4c. A sample at 860.42 m shows very low uranium, 0.8 ppm. The sample at 957.50 m is slightly enriched in uranium and thorium, 7 ppm and 23 ppm, respectively.

The group C metatonalite sample shows normal values, 1.4% potassium, 2 ppm uranium and 7 ppm thorium.

The leucogranite and pegmatitic granite of group D shows typically high content of potassium, uranium and thorium; 4.2 and 4.9% potassium, 8 and 12 ppm uranium, 22 and 38 ppm thorium, respectively. Hence, the natural exposure rate is high, 18 and 26 micro-R/h. However, the relative distribution of the elements falls within normal granite, Figure 7-4c.

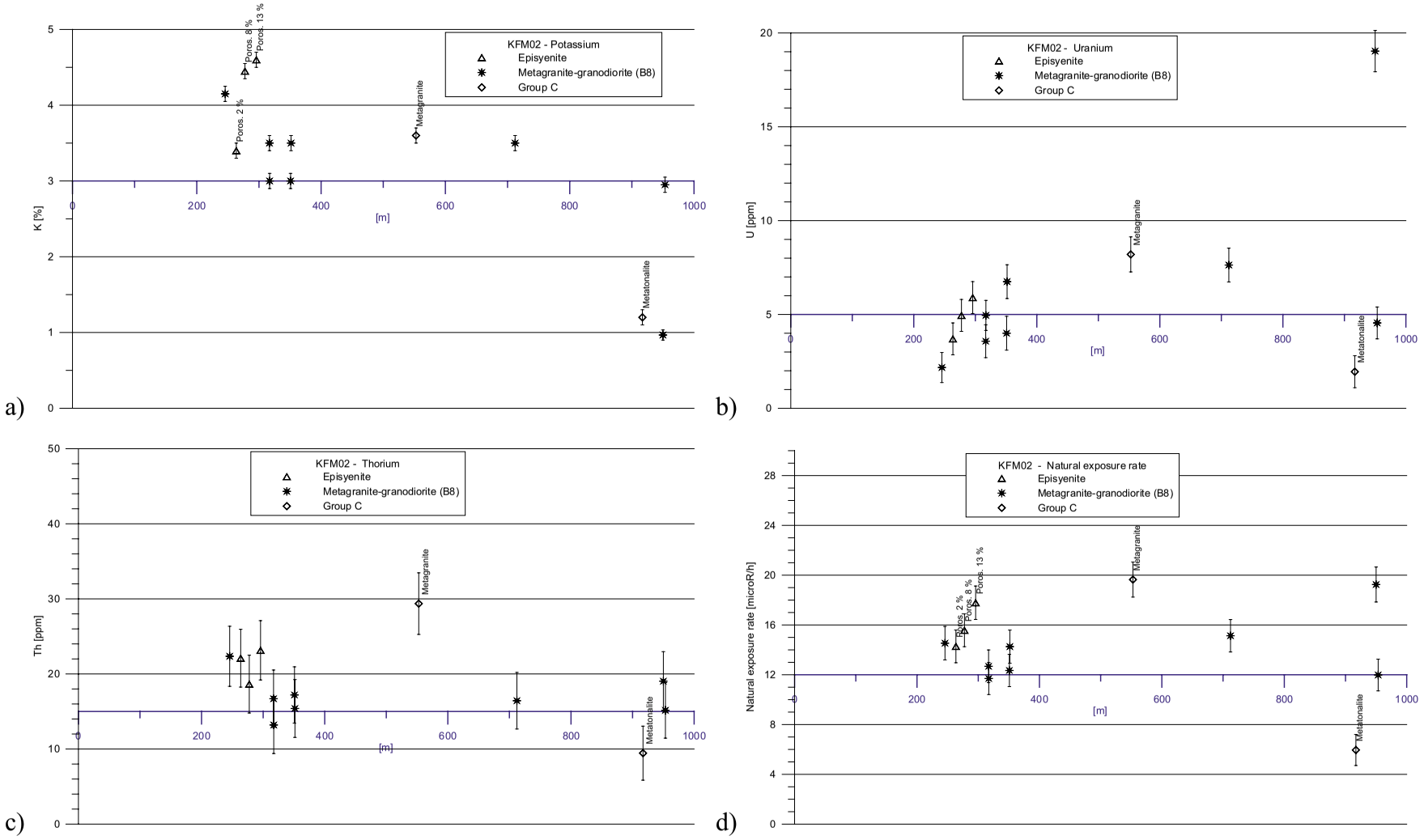

Figure 7-2. *Gamma ray spectrometry data for different rock types, plotted with reference to the borehole depth of KFM02A. a) K content, %. b) U content, ppm. c) Th content, ppm. d) Natural exposure rate, microR/h. Standard error bars are shown. The borehole axis position represents normal levels for granite.*

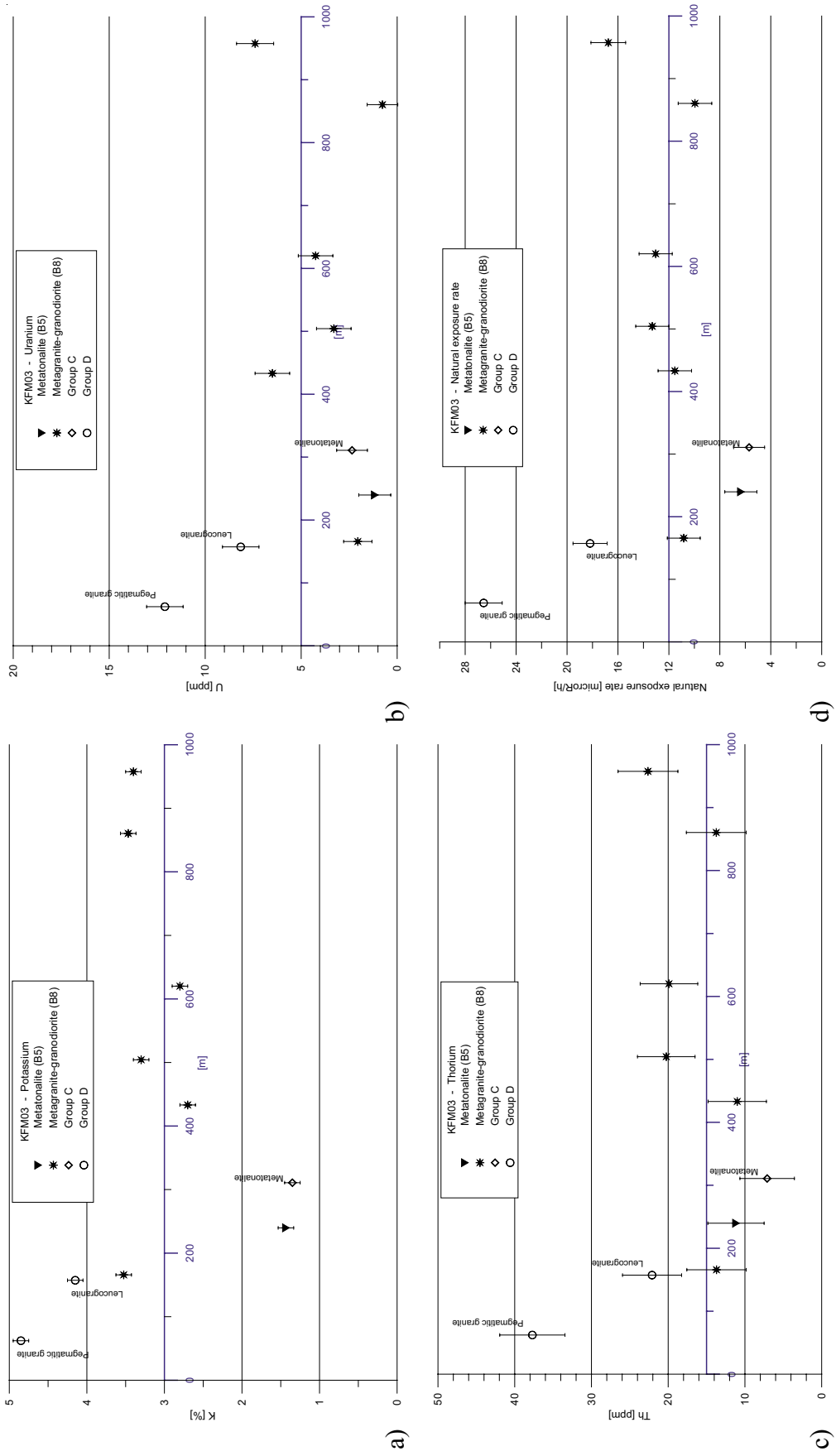

Figure 7-3. *Gamma ray spectrometry data for different rock types plotted with reference to the borehole depth of KFM03A+B. a) K content, %. b) U content, ppm. c) Th content, ppm. d) Natural exposure rate, micro-R/h. Standard error bars are shown. The borehole axis position represents normal levels for granite.*

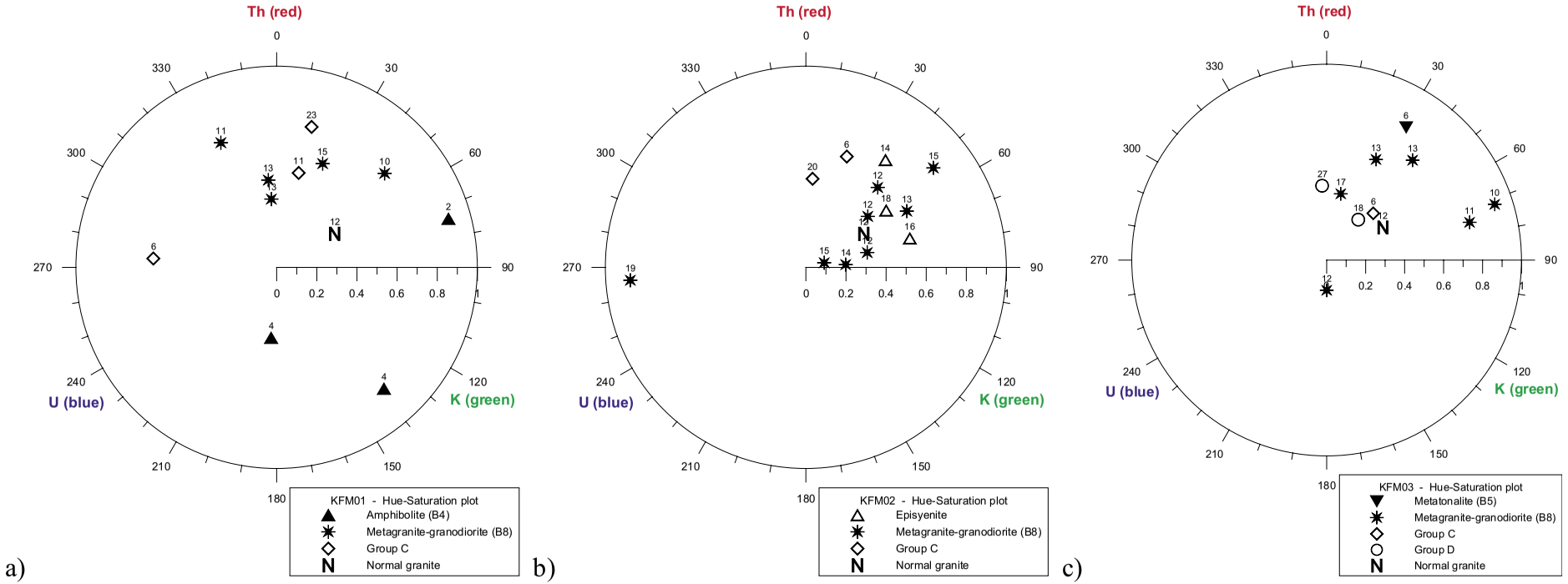

Figure 7-4. *Hue-Saturation plot of gamma ray spectrometry measurements on samples from drillhole KFM01, KFM02 and KFM03. The presentation shows, for different rock types, the relative distribution between potassium, uranium and thorium in uranium equivalent units (Ur). The letter N marks the position for normal distribution in granite (that is, 3% K, 5 ppm U, 15 ppm Th). Digits show the natural exposure in microR/h. a) KFM01 b) KFM02 c) KFM03*

8 Compilation of petrophysical parameters

8.1 Summary of results

In the tables below a compilation of some petrophysical parameters and gamma-ray spectrometry data is presented for each borehole respectively, KFM01A (Table 8-1a,b), KFM02A (Table 8-2a,b) and KFM03 (Table 8-3a,b).

Table 8-1a. Some petrophysical parameters of KFM01A.

Sec up (m)	Sec low (m)	Wet density (kg/m^3)	Poro-sity (%)	Kmean (SI)	Rema-nence intensity (A/m)	Q value (SI)	Resistivity (Ωm) fresh water	IP at 0.1 Hz (mrad) fresh water	Rock group	Results from the petrophysical rock classification (from Figure 4-1)
110.06	110.26	2,663	0.28	0.00946	0.09199	0.237	33,150	5.1	B8/B9	Granite
241.90	242.10	2,713	0.40	0.00039	0.00780	0.487	8,290	7.0	C	Granodiorite
317.80	318.00	2,660	0.29	0.00896	0.08905	0.243	19,870	7.7	B8/B9	Granite
355.10	355.30	2,989	0.24	0.00067	0.00007	0.003	36,690	9.6	B4	Mafic volcanite
474.00	474.20	3,048	0.32	0.00069	0.00005	0.002	18,860	2.7	B4	Mafic volcanite
476.60	476.80	2,678	0.34	0.00026	0.01070	1.014	9,710	6.3	B8/B9	Granite-granodiorite
521.40	521.60	2,688	0.28	0.00033	0.02155	1.603	6,470	4.5	C	Granite-granodiorite
706.00	706.20	2,661	0.29	0.01647	0.08265	0.122	10,770	4.6	B8/B9	Granite
947.80	948.00	2,661	0.36	0.01262	0.21877	0.423	3,870	6.1	B8/B9	Granite
969.90	970.10	2,642	0.47	0.00330	0.01401	0.104	6,050	2.4	C	Granite

Table 8-1b. Gamma-ray spectrometry data from KFM01A.

Sec up (m)	Sec low (m)	K (%)	U (ppm)	Th (ppm)	Natural expo-sure (µR/H)	Rock group	Rock type
109.60	110.06	2.3	5.8	19.2	13.0	B8/B9	Metagranite-granodiorite
242.25	242.55	2.2	4.3	16.6	11.1	C	Meta-granodiorite
315.85	316.25	3.2	5.0	23.0	15.0	B8/B9	Metagranite-granodiorite
355.30	355.50	1.0	2.4	3.1	3.8	B4	Amphibolite
432.96	433.15	1.6	1.7	1.5	3.8	B4	Amphibolite
473.53	473.71	0.8	0.2	2.9	2.1	B4	Amphibolite
477.10	477.50	1.2	5.4	18.0	10.7	B8/B9	Metagranite-granodiorite
521.10	521.40	0.8	4.7	6.9	6.2	C	Metagranodiorite-tonalite
704.69	705.10	2.5	6.3	18.3	13.3	B8/B9	Metagranite-granodiorite
947.40	947.80	2.7	2.2	15.0	10.0	B8/B9	Metagranite-granodiorite
970.10	970.50	4.0	6.0	42.4	22.8	C	Metagranite

Table 8-2a. Some petrophysical parameters of KFM02A.

Sec up (m)	Sec low (m)	Wet density (kg/m^3)	Poro-sity (%)	Kmean (SI)	Rema-nence intensity (A/m)	Q value (SI)	Resistivity (Ωm) fresh water	IP at 0.1 Hz (mrad) fresh water	Rock group	Results from the petrophysical rock classification (from Figure 4-4)
244.40	244.60	2,639	0.66	0.00019	0.00130	0.171	19,570	7.0	B8/B9	Granite
263.15	263.35	2,568	1.97	0.00019	0.00450	0.572	3,610	5.4	Episyenite	No classification
277.90	278.10	2,263	8.47	0.00022	0.01095	1.238	1,280	7.9	Episyenite	No classification
295.45	295.64	2,064	13.06	0.00031	0.02626	2.060	1,060	6.5	Episyenite	No classification
316.63	316.83	2,648	0.53	0.01466	0.14230	0.237	11,860	9.0	B8/B9	Granite
317.45	317.65	2,650	0.46	0.01260	0.06524	0.126	10,240	11.7	B8/B9	Granite
350.60	350.80	2,654	0.44	0.01057	0.06548	0.151	16,600	5.9	B8/B9	Granite
351.00	351.20	2,659	0.31	0.01067	0.06076	0.139	16,580	3.8	B8/B9	Granite
552.43	552.63	2,648	0.38	0.00100	0.00477	0.117	11,360	3.5	C	Granite
712.25	712.45	2,649	0.37	0.00040	0.00195	0.118	10,250	4.6	B8/B9	Granite
915.90	916.10	2,832	0.33	0.00046	0.00454	0.243	11,060	8.5	C	Diorite
949.67	949.87	2,655	0.35	0.02157	0.49025	0.555	4,370	4.8	B8/B9	Granite
953.48	953.68	2,652	0.36	0.01948	0.46113	0.578	4,330	5.5	B8/B9	Granite

Table 8-2b. Gamma-ray spectrometry data from KFM02A.

Sec up (m)	Sec low (m)	K (%)	U (ppm)	Th (ppm)	Natural expo-sure (µR/H)	Rock group	Rock type
245.55	245.75	4.2	2.2	22.4	14.5	B8/B9	Metagranite-granodiorite
263.35	263.68	3.4	3.7	22.1	14.3	Bepi	Episyenite
277.29	277.60	4.5	5.0	18.7	15.6	Bepi	Episyenite
295.64	295.81	4.6	5.9	23.2	17.8	Bepi	Episyenite
316.85	317.05	3.5	3.6	16.7	12.7	B8/B9	Metagranite-granodiorite
317.05	317.45	3.0	5.0	13.2	11.7	B8/B9	Metagranite-granodiorite
350.80	351.00	3.0	4.0	17.2	12.3	B8/B9	Metagranite-granodiorite
351.45	351.85	3.5	6.8	15.4	14.3	B8/B9	Metagranite-granodiorite
552.66	552.86	3.6	8.2	29.4	19.6	C	Metagranite
712.05	712.25	3.5	7.6	16.4	15.1	B8/B9	Metagranite-granodiorite
916.85	917.05	1.2	2.0	9.5	6.0	C	Metatonalite
949.90	950.10	1.0	19.0	19.0	19.3	B8/B9	Metagranite-granodiorite
953.25	953.45	3.0	4.6	15.2	12.0	B8/B9	Metagranite-granodiorite

Table 8-3a. Some petrophysical parameters of KFM03A and KFM03B.

Sec up (m)	Sec low (m)	Wet density (kg/m³)	Poro-sity (%)	Kmean (SI)	Rema-nence intensity (A/m)	Q value (SI)	Resistivity (Ωm) fresh water	IP at 0.1 Hz (mrad) fresh water	Rock group	Results from the petrophysical rock classification (from Figure 4-7)
60.46	60.66	2,637	0.59	0.00019	0.00046	0.061	11,790	13.0	D2	Granite
157.00	157.20	2,627	0.69	0.00573	0.00733	0.031	7,920	5.2	D?	Granite
165.50	165.70	2,656	0.38	0.00908	0.04101	0.110	13,820	4.1	B8/B9	Granite
239.44	239.64	2,786	0.45	0.00037	0.00087	0.058	7,500	3.1	B5	Tonalite-diorite
310.49	310.75	2,810	0.33	0.00045	0.00232	0.127	8,260	3.9	C	Tonalite-diorite
432.75	432.95	2,654	0.43	0.01295	0.43080	0.812	10,460	3.5	B8/B9	Granite
504.00	504.20	2,655	0.45	0.00878	0.07020	0.195	7,590	3.2	B8/B9	Granite
619.80	620.00	2,651	0.58	0.00017	0.00961	1.414	8,130	4.5	B8/B9	Granite
856.82	857.02	2,654	0.51	0.01337	0.06058	0.111	7,540	2.8	B8/B9	Granite
957.20	957.40	2,650	0.50	0.00952	0.04029	0.103	34,320	7.5	B8/B9	Granite

Table 8-3b. Gamma-ray spectrometry data from KFM03A and KFM03B.

Sec up (m)	Sec low (m)	K (%)	U (ppm)	Th (ppm)	Natural expo-sure (μR/H)	Rock group	Rock type
62.09	62.28	4.9	12.1	37.7	26.5	D2	Pegmatitic granite
157.20	157.40	4.2	8.2	22.1	18.2	D?	Leucogranite
165.70	165.90	3.5	2.1	13.7	10.8	B8/B9	Metagranite-granodiorite
239.64	239.84	1.4	1.2	11.2	6.3	B5	Metatonalite
310.75	310.96	1.4	2.4	7.1	5.7	C	Metatonalite
433.07	433.27	2.7	6.5	11.0	11.5	B8/B9	Metagranite-granodiorite
504.20	504.40	3.3	3.3	20.3	13.3	B8/B9	Metagranite-granodiorite
620.00	620.20	2.8	4.3	19.9	13.0	B8/B9	Metagranite-granodiorite
860.32	860.52	3.5	0.8	13.7	10.0	B8/B9	Metagranite-granodiorite
957.40	957.60	3.4	7.4	22.6	16.8	B8/B9	Metagranite-granodiorite

Selected parameters (averages) for the only rock group (metagranite-granodiorite) that have sufficient amount of data, > 10 samples, to form the basis of a statistical conclusion, is presented in Table 8-4. Further processing and evaluation as well as co-interpretation between the different properties will be made when more data are available.

Table 8-4. Compilation of petrophysical parameters for B8/B9, metagranodiorite to metagranite. Resistivity and IP measured at 0.1 Hz in fresh water (~ 42 Ωm). (* based on 19 gamma-ray spectrometry samples).

Rock group Unit	Volume susceptibility SI	Q-value SI	Density kg/m³	Porosity %	Resistivity Ωm	IP mrad	K * %	U * ppm	Th * ppm	Natural exposure * μR/H
B8/B9	0.010	0.36	2,655	0.41	11,120	5.6	2.9	5.3	17.4	13.1

8.2 Comments on the results

Some evident results from the petrophysical investigation are commented below:

- Vuggy granite/episyenite samples have high porosity, low density, low magnetic susceptibility and low resistivity.
- Vuggy granite/episyenite samples have a relation between resistivity and porosity that indicates presence of vugs, constrictions, dead-end pores and/or crocked path-ways.
- Resistivity in fresh water is strongly dependent upon surface conductivity. Samples with fine-grained phyllosilicates seem to have the lowest resistivities, vuggy granite/ episyenite samples excluded.
- The median porosity is highest in KFM03A and lowest in KFM01A.
- The magnetic fabric orientations and the dip of the NRM vectors of KFM03 clearly deviate from those of KFM01 and KFM02, with shallow to moderate dips of the foliation in KFM03 compared to moderate to steep dips in KFM01 and KFM02.
- A metagranite sample of KFM01A (depth c 476 m) has a significantly lower magnetic susceptibility but a slightly higher density than the other metagranite samples in this borehole.
- The metagranite-granodiorite, in general, display normal contents for granite that is in average; 2.9% potassium, 5 ppm uranium and 17 ppm thorium. For other rock types the number of samples is too low to allow statistical conclusions.
- The episyenite samples and a metagranite-granodiorite sample close to the episyenite, in the upper part of KFM02A, show a relative enrichment in potassium and thorium, 4.2–4.6% K and 19 – 23 ppm Th, respectively.
- Some metagranite samples belonging to group C show high thorium levels, 29 and 42 ppm.
- A leucogranite and a pegmatite granite sample in KFM03 show typically high content of potassium, uranium and thorium.

9 Data delivery

The processed data and interpretation results have been delivered to SKB. The SICADA field note no is Forsmark 336.

All data have been documented according to “GIS – Inleverans av data”, SKB SD-081 (SKB internal controlling document).

10 References

/1/ **Mattsson H, Isaksson H, Thunehed H, 2003.** Petrophysical rock sampling, measurements of petrophysical rock parameters and in situ gamma ray spectrometry measurements on outcrops carried out 2002. SKB P-03-26. Svensk Kärnbränslehantering AB.

/2/ **Pettersson J, Tullborg E-L, Berglund J, Lindroos H, Danielsson P, Wängnerud A, Mattsson H, Thunehed H, Isaksson H.** Petrography, geochemistry, petrophysics and fracture mineralogy of boreholes KFM01A, KFM02A and KFM03A+B. SKB P-04-103. Svensk Kärnbränslehantering AB.

/3/ **Henkel H, 1991.** Petrophysical properties (density and magnetization of rock from the northern part of the Baltic Shield). Tectonophysics 192, page1–19.

/4/ **Collinson D W, 1983.** Methods in rock magnetism and paleomagnetism, Chapman and Hall, London, United Kingdom. 503 pp.

/5/ **Parasnis D S, 1997.** Principles of applied geophysics. Chapman and Hall, London, 429 pp.

/6/ **Puranen R, 1989.** Susceptibilities, iron and magnetite content of Precambrian rocks in Finland. Geological survey of Finland, Report of investigations 90, 45 pp.

/7/ **Isaksson H, Mattsson H, Thunehed H, Keisu M.** Interpretation of petrophysical surface data Stage 1 (2002). SKB P-03-102. Svensk Kärnbränslehantering AB.

/8/ **Tarling D H, Hrouda F, 1993.** The magnetic anisotropy of rocks, Chapman and Hall, London, United Kingdom. 217 pp.

/9/ **Archie G E, 1942.** The electrical resistivity log as an aid in determining some reservoir characteristics: Trans Am Inst Min, Metallurg, Petr Eng, 146, 54–62.

/10/ **Keller G V, Frischknecht F C, 1966.** Electrical methods in geophysical prospecting. Pergamon Press.

/11/ **Mattson H, Thunehed H, 2004.** Interpretation of geophysical borehole data and compilation of petrophysical data from KSH02 (80–1,000 m) and KAV01. SKB P-04-77. Svensk Kärnbränslehantering AB.

/12/ **Grasty R L, Carson J M, Charbonneau B W, Holman P B, 1984.** Natural Background Radiation in Canada; Geological Survey of Canada, Bulletin 360, 39 p.

/13/ **Möller C, Snäll S, Stephens M B, 2003.** Dissolution of quartz, vug formation and new grain growth associated with post-metamorphic hydrothermal alteration in KFM02A. SKB P-03-77. Svensk Kärnbränslehantering AB, 56 pp.

Gamma-ray spectrometry, laboratory measurements

Appendix 1

Drillhole ID	Secup (m)	Seclow (m)	SGU ID	No of measure-ments	K mean (%)%	K max (%)	K min (%)	Diff. From mean (%)	U mean (ppm)	U max (ppm)	U min (ppm)	Diff. From mean (%)	Th mean (ppm)	Th max (ppm)	Th min (ppm)	Diff. From mean (%)	K mean error	U mean error	Th mean error	Gamma index	Natural exposure µR/h
KFM01A	109.6	110.06	skb12	2	2.3	2.4	2.1	6.7	5.8	7.0	4.6	20.7	19.2	20.8	17.6	8.3	0.1	0.9	3.8	0.86	13.0
KFM01A	242.25	242.55	skb79	2	2.2	2.2	2.1	2.3	4.3	4.5	4.1	4.7	16.6	16.6	16.6	0.0	0.1	0.9	3.9	0.74	11.1
KFM01A	315.85	316.25	skb26	2	3.2	3.3	3	4.8	5.0	6.3	3.7	26.0	23.0	27.8	18.1	21.1	0.1	0.9	3.9	1.00	15.0
KFM01A	355.3	355.5	skb28	2	1.0	1.1	0.8	15.8	2.4	4.3	0.4	83.0	3.1	6.1	0.0	100.0	0.1	0.8	3.4	0.26	3.8
KFM01A	432.96	433.15	skb77	2	1.6	1.6	1.5	3.2	1.7	3.3	0.0	100.0	1.5	2.9	0.0	100.0	0.1	0.8	3.6	0.26	3.8
KFM01A	473.53	473.71	skb9	2	0.8	1	0.5	33.3	0.2	0.3	0.1	50.0	2.9	5.7	0.0	100.0	0.1	0.8	3.4	0.14	2.1
KFM01A	477.1	477.5	skb34	2	1.2	1.2	1.2	0.0	5.4	6.0	4.7	12.1	18.0	18.7	17.3	3.9	0.1	0.9	3.9	0.71	10.7
KFM01A	521.1	521.4	skb82	2	0.8	0.8	0.7	6.7	4.7	5.5	3.9	17.0	6.9	7.9	5.9	14.5	0.1	4.4	3.6	0.41	6.2
KFM01A	704.69	705.1	skb81	2	2.5	2.5	2.5	0.0	6.3	6.9	5.6	10.4	18.3	21.6	14.9	18.4	0.1	0.9	3.8	0.89	13.3
KFM01A	947.4	947.8	skb33	2	2.7	2.8	2.6	3.7	2.2	2.8	1.5	30.2	15.0	17.9	12.0	19.7	0.1	0.9	3.8	0.67	10.0
KFM01A	970.1	970.5	skb80	2	4.0	4	3.9	1.3	6.0	6.9	5.0	16.0	42.4	43.3	41.5	2.1	0.1	0.9	4.4	1.51	22.8
KFM02A	245.55	245.75	skb56C	4	4.2	4.4	4	4.8	2.2	4.0	0.0	92.0	22.4	25.0	17.5	16.8	0.1	0.8	4.0	0.97	14.5
KFM02A	263.35	263.68	skb10	2	3.4	3.4	3.4	0.0	3.7	5.0	2.4	35.1	22.1	23.7	20.5	7.2	0.1	0.9	3.9	0.95	14.3
KFM02A	277.29	277.6	skb19	2	4.5	4.8	4.1	7.9	5.0	5.7	4.2	15.2	18.7	24.0	13.3	28.7	0.1	0.9	3.9	1.04	15.6
KFM02A	295.64	295.81	skb17	2	4.6	5	4.2	8.7	5.9	7.7	4.1	30.5	23.2	24.6	21.7	6.3	0.1	0.9	4.0	1.19	17.8
KFM02A	316.85	317.05	skb3C	4	3.5	3.8	3.3	7.1	3.6	4.9	2.4	35.0	16.7	18.7	14.4	12.9	0.1	0.9	3.8	0.85	12.7
KFM02A	317.05	317.45	skb16	2	3.0	3.3	2.7	10.0	5.0	6.1	3.8	23.2	13.2	13.2	13.2	0.0	0.1	0.8	3.8	0.78	11.7
KFM02A	350.8	351	skb24	2	3.0	3	3	0.0	4.0	4.5	3.5	12.5	17.2	19.2	15.2	11.6	0.1	0.9	3.8	0.82	12.3
KFM02A	351.45	351.85	skb14	2	3.5	3.5	3.5	0.0	6.8	6.8	6.7	0.7	15.4	18.0	12.8	16.9	0.1	0.9	3.9	0.95	14.3
KFM02A	552.66	552.86	skb20	3	3.6	3.8	3.5	4.2	8.2	9.3	6.1	19.5	29.4	30.1	28.1	3.4	0.1	0.9	4.1	1.31	19.6
KFM02A	712.05	712.25	skb21	3	3.5	3.5	3.5	0.0	7.6	8.9	7.0	12.4	16.4	19.3	15.0	13.1	0.1	0.9	3.8	1.01	15.1
KFM02A	916.85	917.05	skb13	2	1.2	1.2	1.2	0.0	2.0	2.4	1.5	23.1	9.5	10.9	8.0	15.3	0.1	0.9	3.6	0.40	6.0
KFM02A	949.9	950.1	skb5	3	1.0	1	0.9	5.2	19.0	20.6	18.1	6.6	19.0	24.4	15.7	22.9	0.1	1.1	3.9	1.27	19.3
KFM02A	953.25	953.45	skb22	2	3.0	3	2.9	1.7	4.6	5.0	4.1	9.9	15.2	16.6	13.7	9.6	0.1	0.9	3.7	0.80	12.0
KFM03A	157.2	157.4	skb25	2	4.2	4.3	4	3.6	8.2	8.8	7.5	8.0	22.1	22.5	21.7	1.8	0.1	1.0	3.9	1.21	18.2
KFM03A	165.7	165.9	skb57C	4	3.5	4.1	3.1	14.2	2.1	3.9	0.3	87.8	13.7	16.5	11.0	20.1	0.1	0.7	3.9	0.73	10.8
KFM03A	239.64	239.84	skb1	3	1.4	1.6	1.2	14.0	1.2	1.5	0.9	25.7	11.2	11.9	10.6	5.8	0.1	0.8	3.7	0.42	6.3
KFM03A	310.75	310.96	skb11	2	1.4	1.5	1.2	11.1	2.4	3.2	1.5	36.2	7.1	8.1	6.1	14.1	0.1	0.8	3.6	0.38	5.7
KFM03A	433.07	433.27	skb15	2	2.7	2.9	2.5	7.4	6.5	7.0	6.0	7.7	11.0	12.4	9.6	12.7	0.1	0.9	3.8	0.77	11.5
KFM03A	504.2	504.4	skb23	2	3.3	3.3	3.3	0.0	3.3	3.7	2.9	12.1	20.3	22.0	18.5	8.6	0.1	0.9	3.8	0.89	13.3
KFM03A	620	620.2	skb2	2	2.8	2.8	2.8	0.0	4.3	5.0	3.5	17.6	19.9	21.2	18.6	6.5	0.1	0.9	3.8	0.87	13.0
KFM03A	860.32	860.52	skb58C	3	3.5	3.7	3.3	5.8	0.8	1.7	0.0	110.9	13.7	17.2	11.6	20.4	0.1	0.8	3.9	0.67	10.0
KFM03A	957.4	957.6	skb4	3	3.4	3.6	3.2	5.9	7.4	8.5	6.7	12.2	22.6	23.3	22.1	2.7	0.1	1.0	3.9	1.12	16.8
KFM03B	62.09	62.28	skb18	2	4.9	5	4.7	3.1	12.1	12.3	11.9	1.7	37.7	39.5	35.9	4.8	0.1	1.0	4.3	1.76	26.5